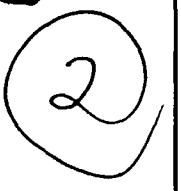

FINAL REPORT: Award N0001490J1245; 11/01/89 - 3/31/94

Title of Project: "Prediction of Deck Wetness on Ships in Motion Through Waves at Finite Forward Speed by Means of a Nonlinear Version of the Slender Ship Theory"

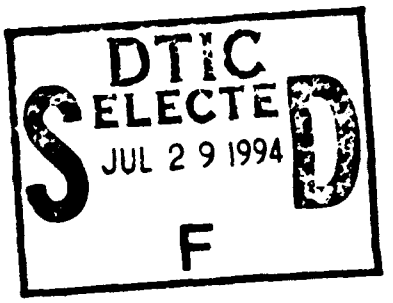

ONR Program Officer: Dr. James Fein

UCSB Principal Investigators: Prof. Marshall Tulin; Prof. Hajime Maruo

Reports

Technical progress has been reported in writing to the Program Officer as required on 10/16/90, 10/16/91, 9/8/92, and 10/6/93. See References (1)-(4). In addition, detailed analyses and results were provided in 1990, 1991, and 1992, see References (5)-(7).

Contractors Meetings

Oral presentations of technical material developed under this contract have been made by Professor Tulin at the following meetings organized by the Program Manager: April 1990 in Washington; Spring 1991 at Berkeley; Spring 1992 at MIT; Spring 1993 at Michigan.

Presentations at Engineering Conferences

Presentations of work developed under this contract have been or will be made as follows:

1991 International Conference on Industrial and Applied Mathematics, Washington, D.C., by Prof. Maruo.

1993 ISOPE Conference, Singapore, by Wusheng Song and Hajime Maruo.

1994 International Conference on Waves and Floating Bodies, Fukuoku, Japan, by Prof. Tulin.

1994 (August) 20th ONR Symposium on Naval Hydrodynamics, Santa Barbara, CA., by Prof. Maruo.

Publications

Work supported by this contract have (or will) appear as References (8)-(11).

Brief Summary of Accomplishments

1. A non-linear theory for the sea response at the bow of ships pitching and heaving in head seas has been systematically derived.

2. This theory has been reduced to non-linear computations of the free surface in the transverse plane, as a function of time (2D&T).

3. The integral equations describing the motion in the transverse plane have been formulated.

4. The problem at the interaction of the free surface and the ship hull was successfully dealt with (this has been a difficulty for some other investigators).

5. A computer method for the solution of these integral equations in time has been formulated, and a code prepared.

6. Calculations have been successfully made, see Enclosures A & B.

7. The method is able to predict the history of water level along the bow, including bow emergence, slamming, and the height of water over the deckline. These are strongly effected by non-linear processes.

References

1. Annual Letter Report for FY 90, from Prof. Marshall P. Tulin, UCSB to Dr. James Fein, ONR.

2. Annual Letter Report for FY 91, from Prof. Marshall P. Tulin, UCSB to Dr. James Fein, ONR.

3. Annual Letter Report for FY 92 from Prof. Marshall P. Tulin, UCSB to Dr. James Fein, ONR.

4. Annual Letter Report for FY 93 from Prof. Marshall P. Tulin, UCSB to Dr. James Fein, ONR.

5. OEL Report 90-53, "Prediction of Deck Wetness: A Theoretical Development," by H. Maruo, August 1990.

6. OEL Report 91-61, "Prediction of Deck Wetness on Ships in Motion Through Waves at Finite Forward Speed by Means of a Nonlinear Version of the Slender Ship Theory," by Hajime Maruo and Wusheng Song, October 1991.

7. OEL Report 92-76, "Treatment of Corners on the 2-D Boundary and Numerical Examples of Nonlinear Deck Wetness," by Wusheng Song, September 1992.

8. OEL Report 94-104, "Nonlinear Analysis of Bow Wave Breaking and Deck Wetness," by Hajime Maruo and Wusheng Song, March 1994.

9. Song, W. and Maruo, H.. "Bow Impact and Deck Wetness: Simulations Based on Nonlinear Slender Body Theory," Proceedings of the 1993 ISOPE Conference, Singapore, June 1993.

10. Tulin, M. and Wu, Ming. "Non-linear Bow Waves on an Inclined Wedge," Proceedings of the 1994 Workshop on Waves and Bodies, Kyushu, Japan.

11. Maruo, H. and Song, W. "Non-linear Analysis of Bow Breaking and Deck Wetness of a High Speed Ship by the Parabolic Approximation," Proceedings of the 20th ONR Symposium on Naval Hydrodynamics, Santa Barbara, August 1994 (to appear).

12. Wu, Ming. Doctoral Dissertation (to appear in early 1995).

Enclosure A

Summary of Material Prepared at UCSB During 1992-93

By

Ming Wu and Professor Marshall P. Tulin

Encl. A.1

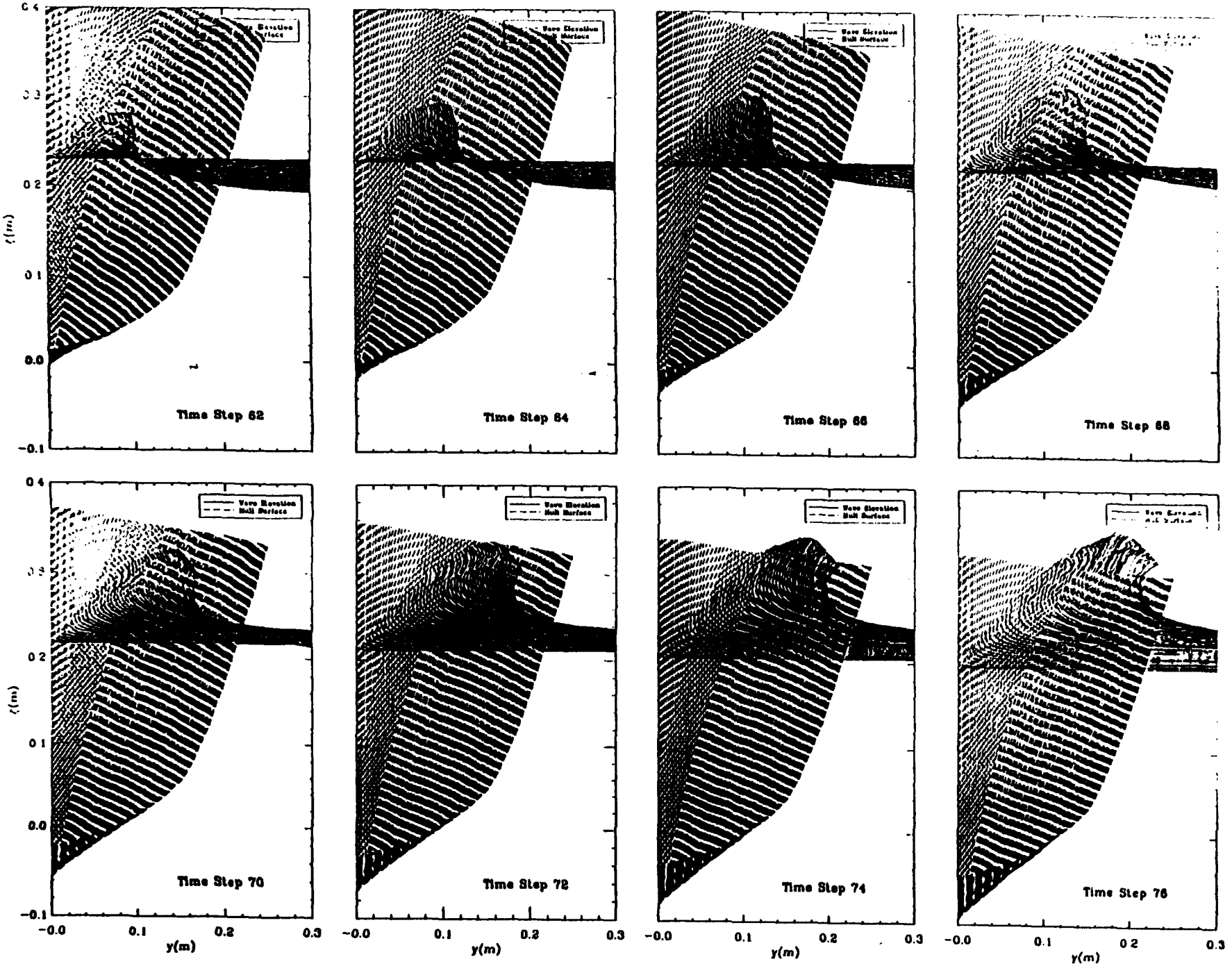

Wave Generated At Bow of a Frigate, $\lambda/Lpp=1.2$, $H/\lambda=0.025$, $Fn=0.3$

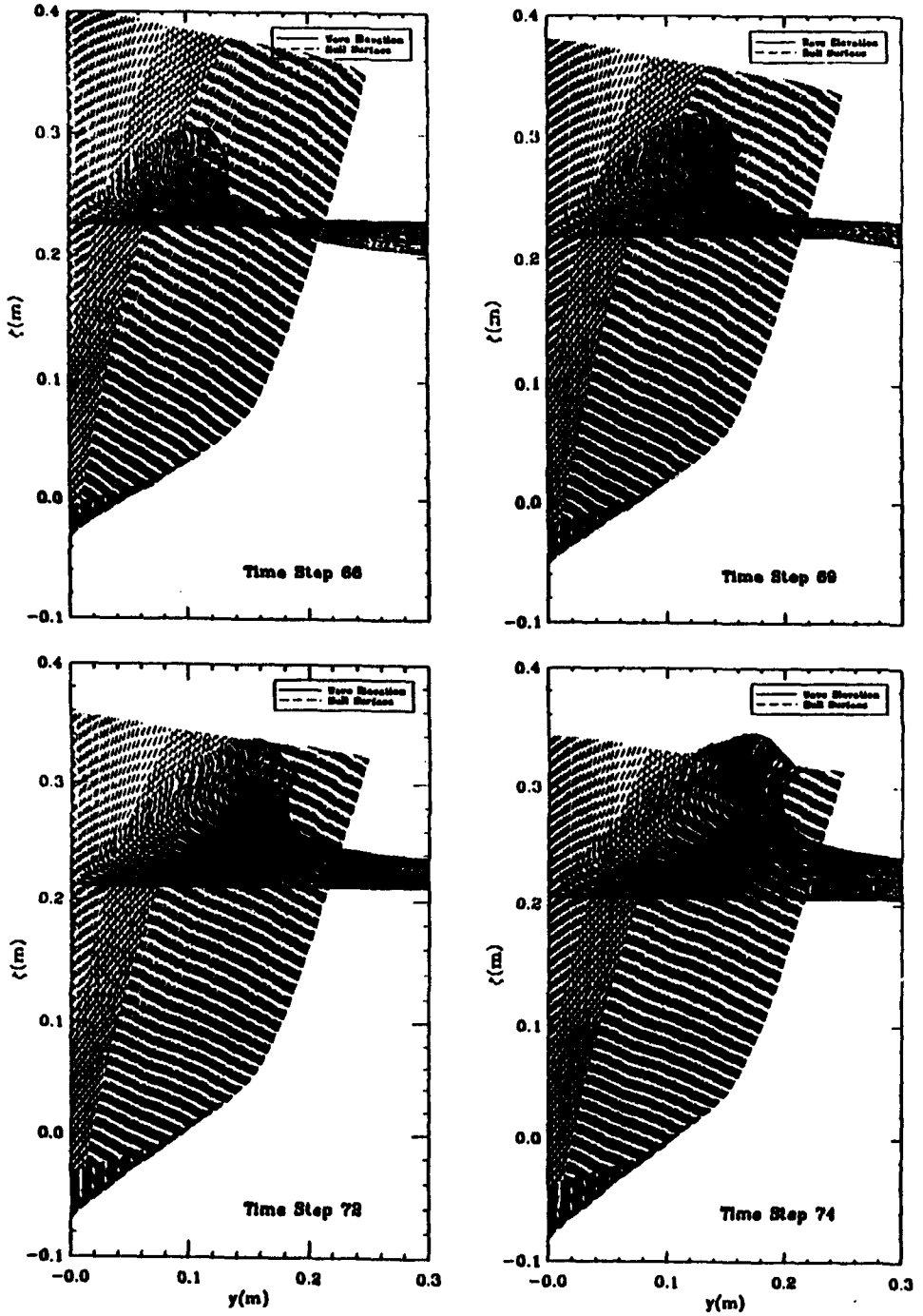

Wave Generated At Bow, $\lambda/Lpp=1.2$, $H/\lambda=0.025$, $Fn=0.3$

Frigate: $H/\lambda = 0.025$; $Fn = 0.30$

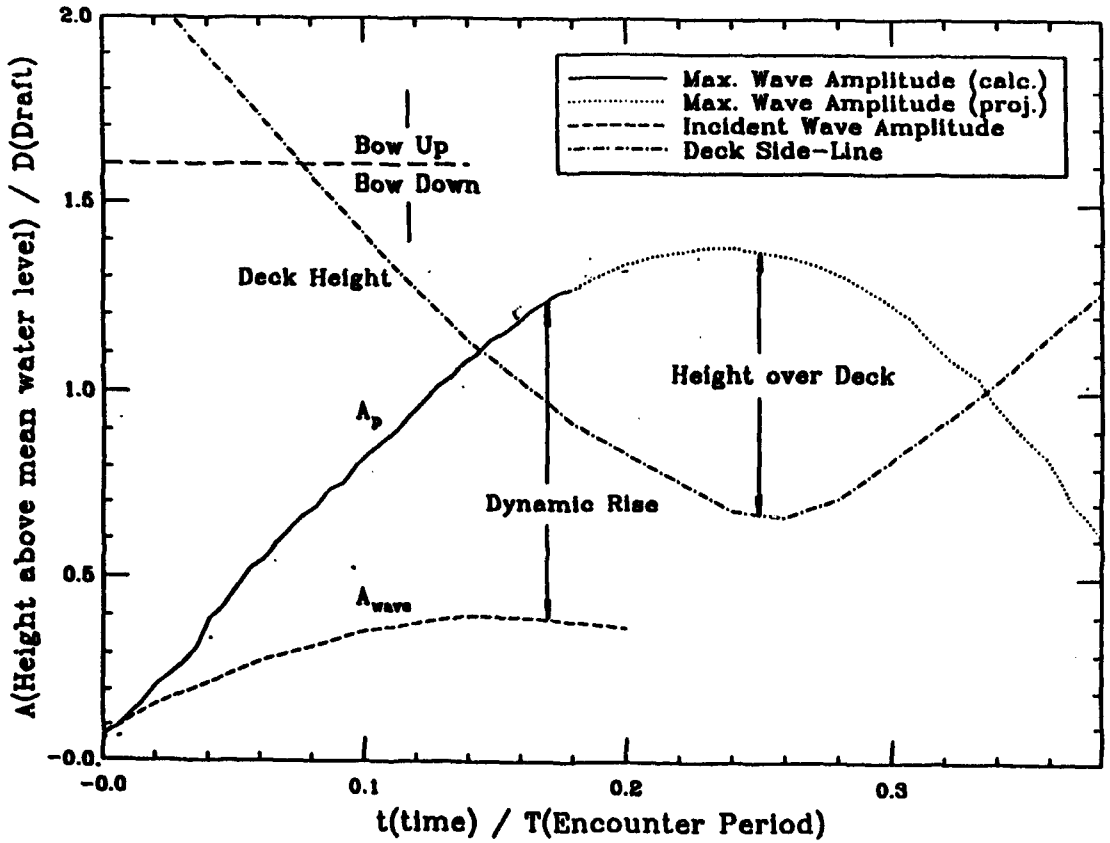

Peak water elevation, A_p, computed in time using non-linear slender body theory

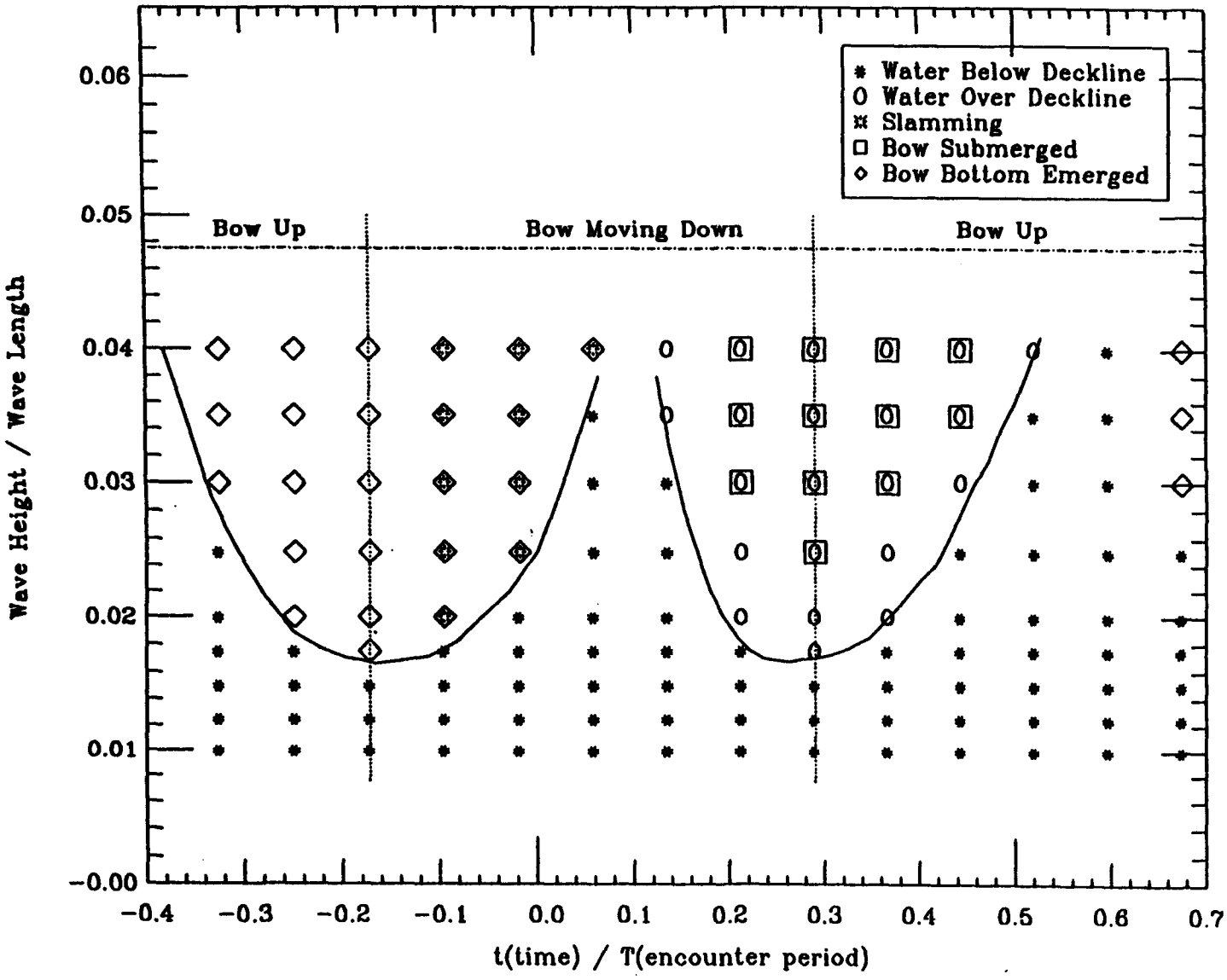

Deck Wetness, Slamming, vs. Wave Parameters

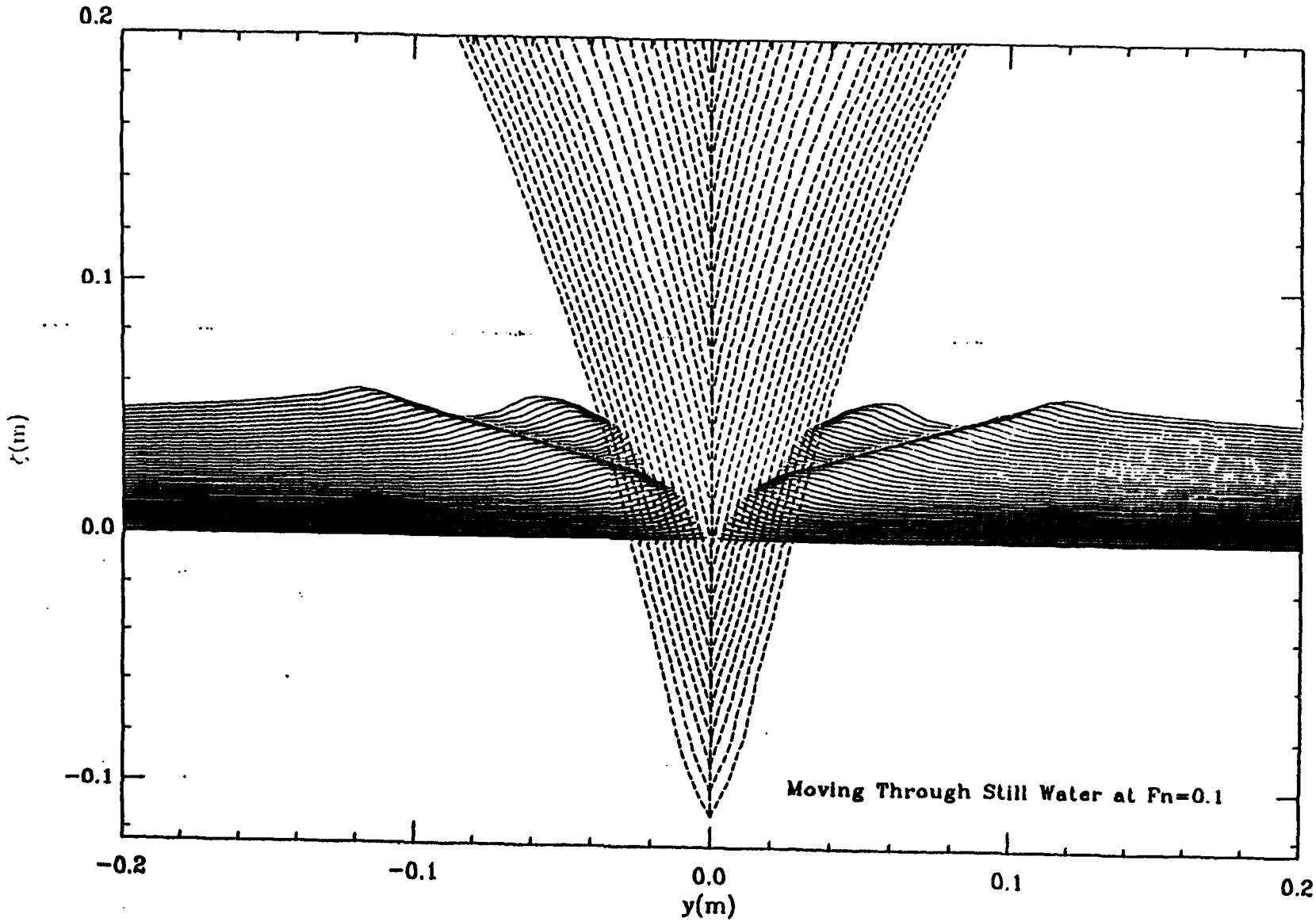

Bow Wave Produced by a Frigate Model

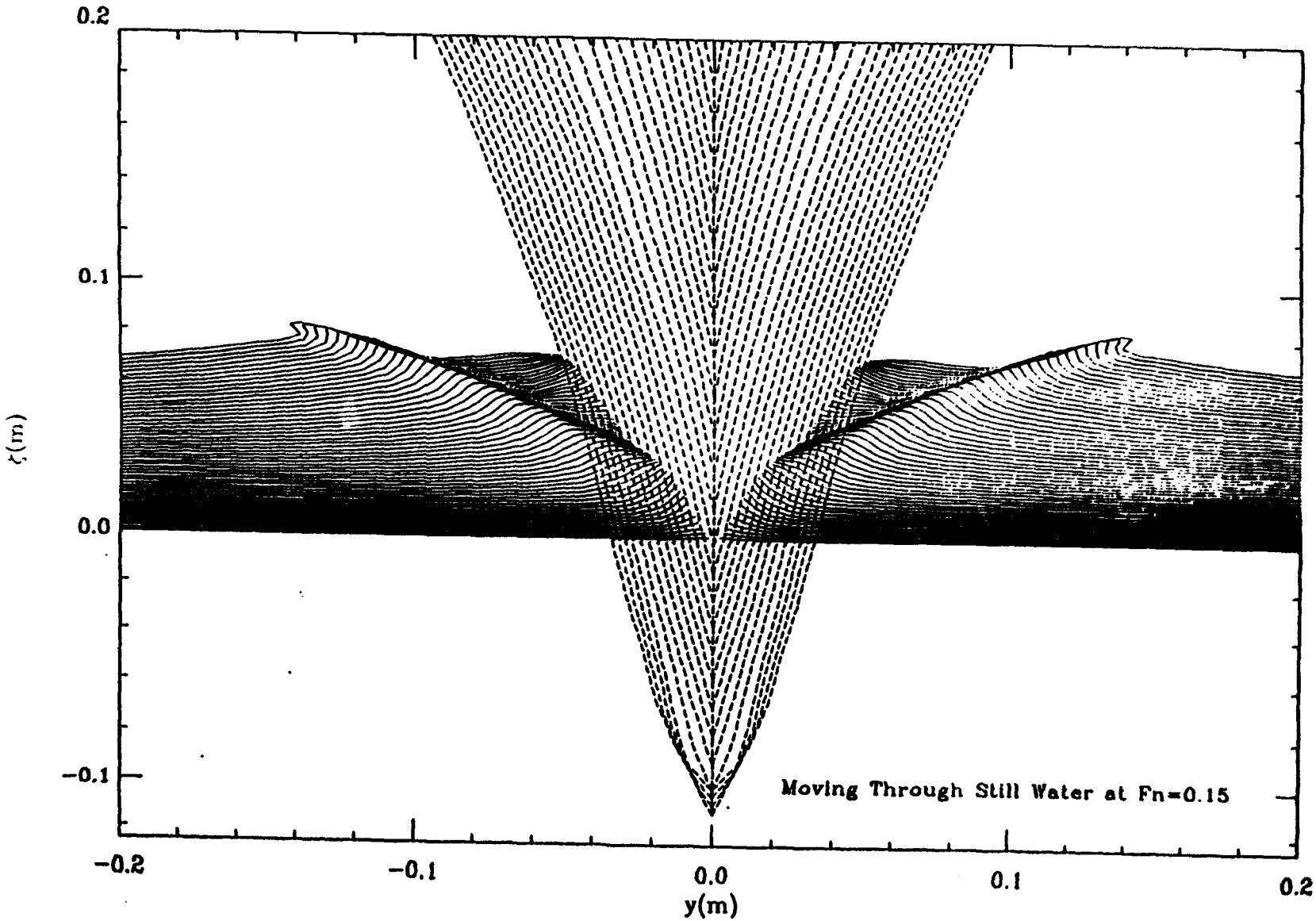

Bow Wave Produced by a Frigate Model

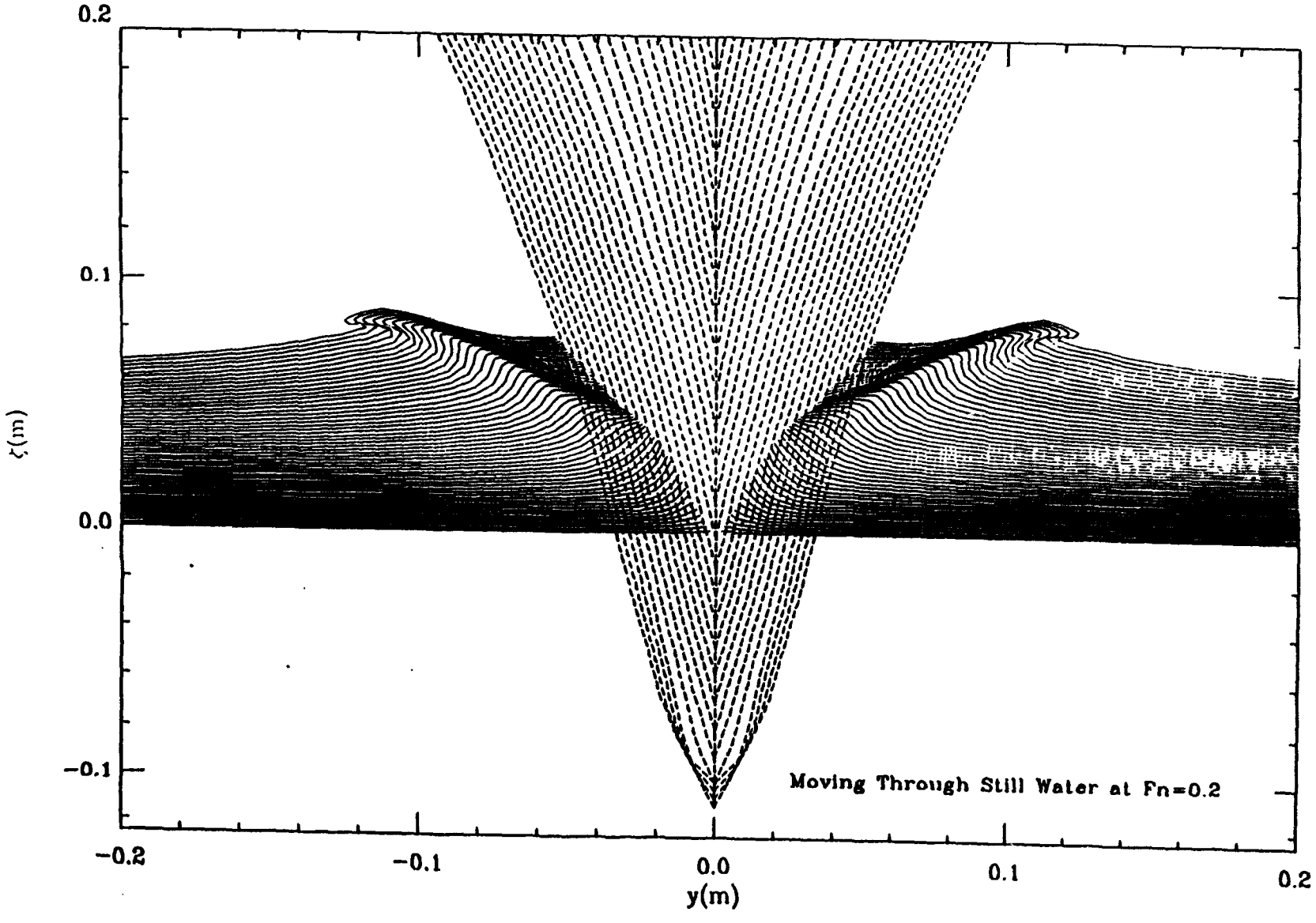

Bow Wave Produced by a Frigate Model

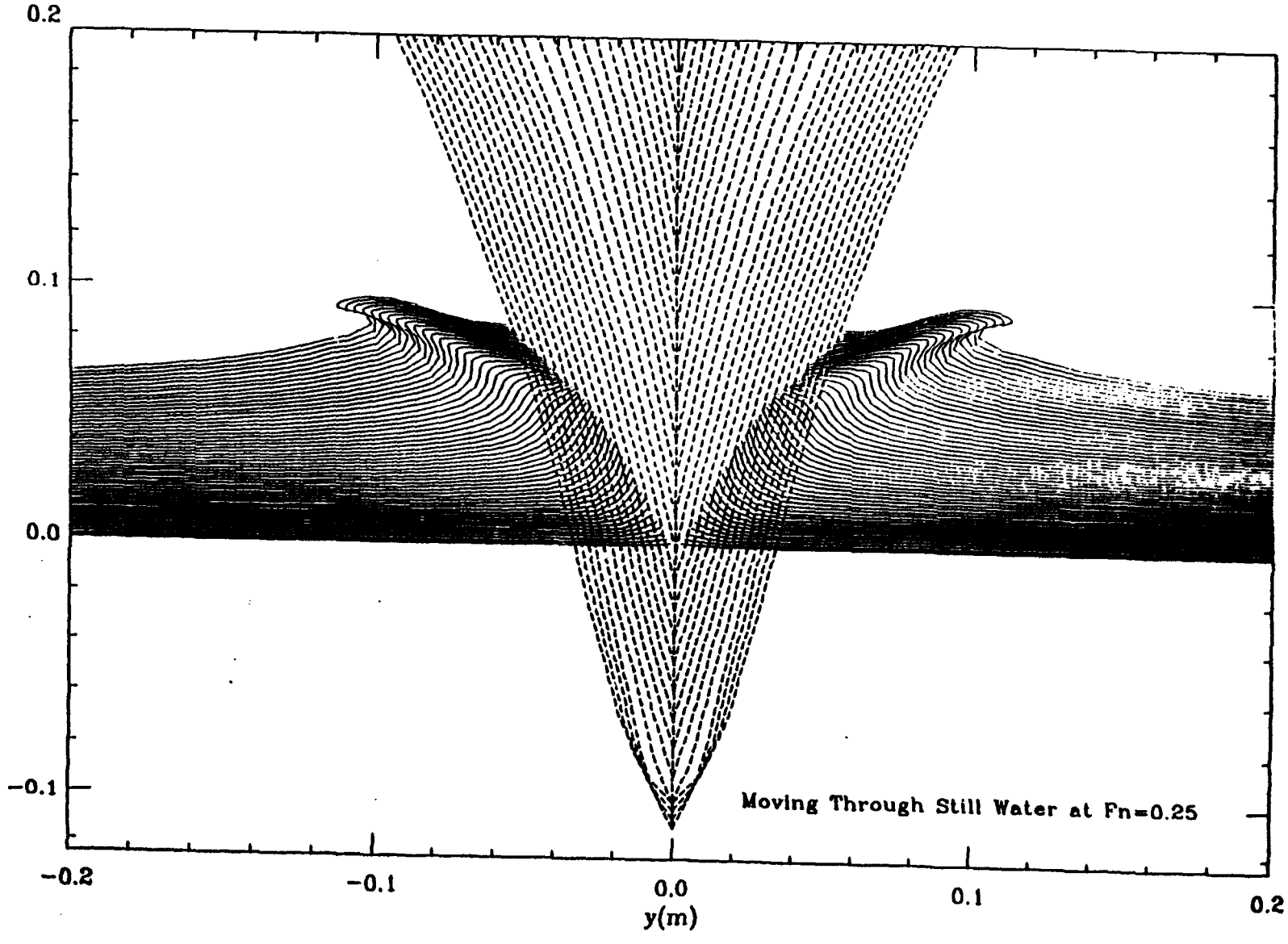

Bow Wave Produced by a Frigate Model

Encl. 0.5

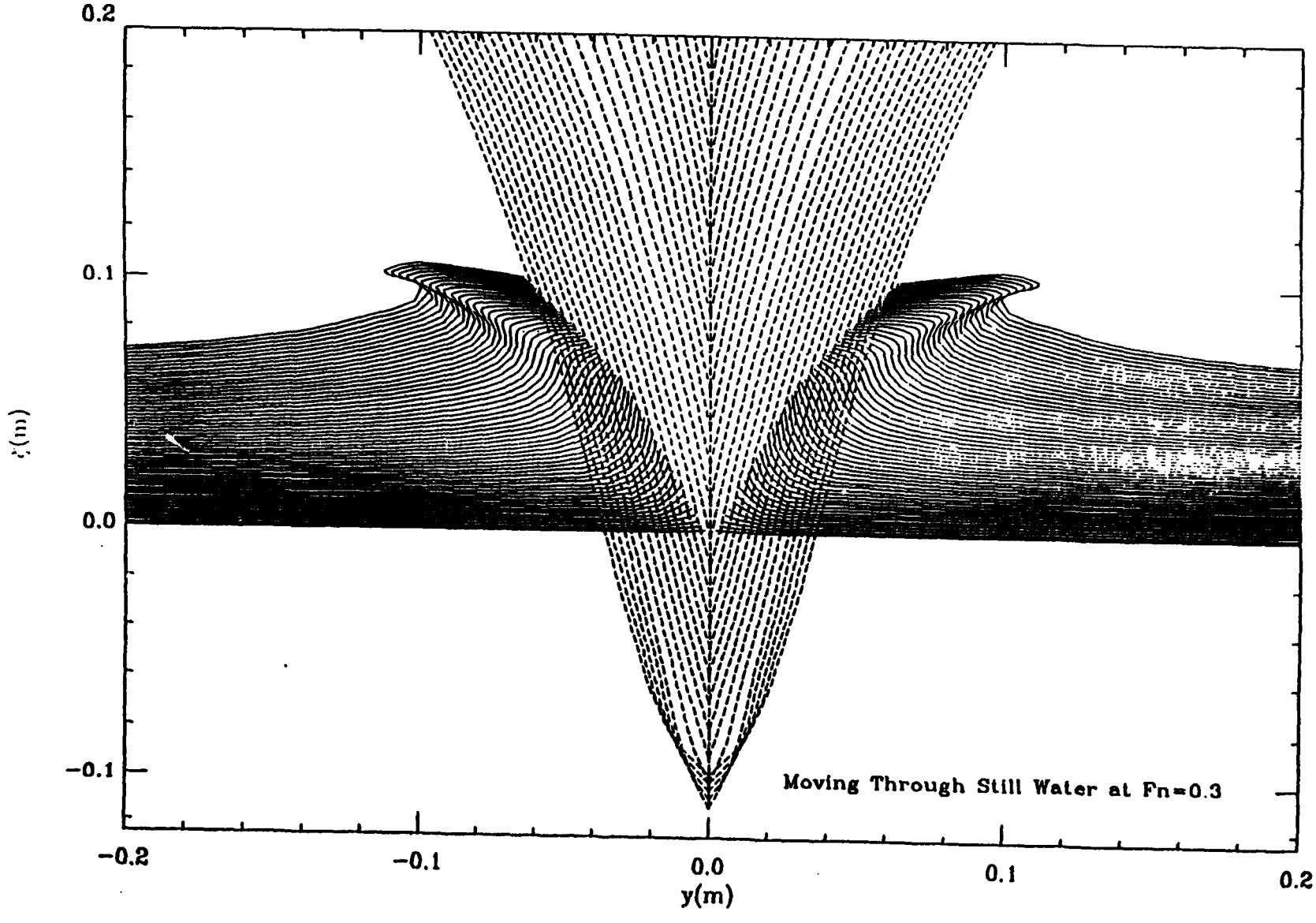

Bow Wave Produced by a Frigate Model

Encl 0.6

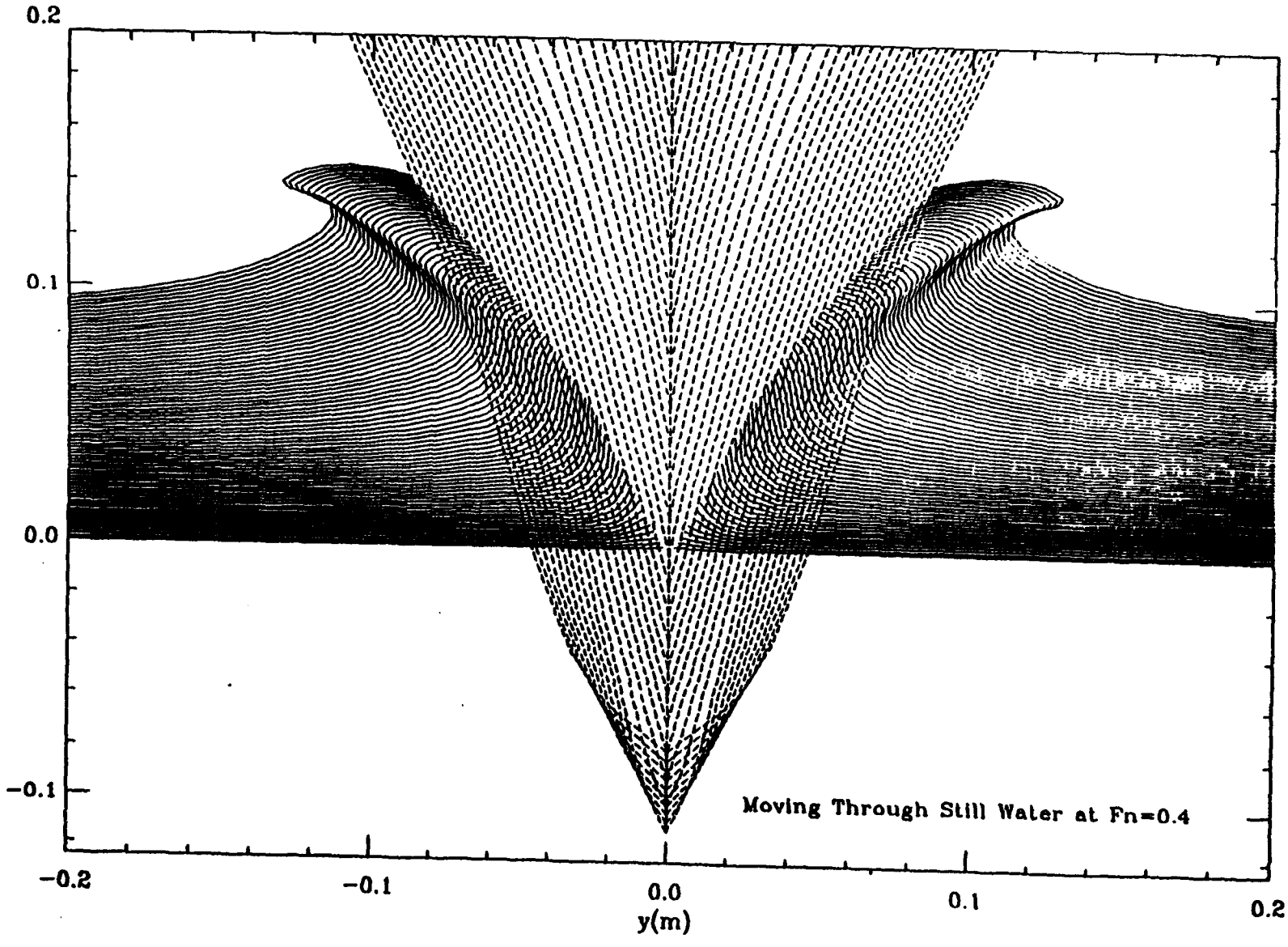

Bow Wave Produced by a Frigate Model

Encl. D.7

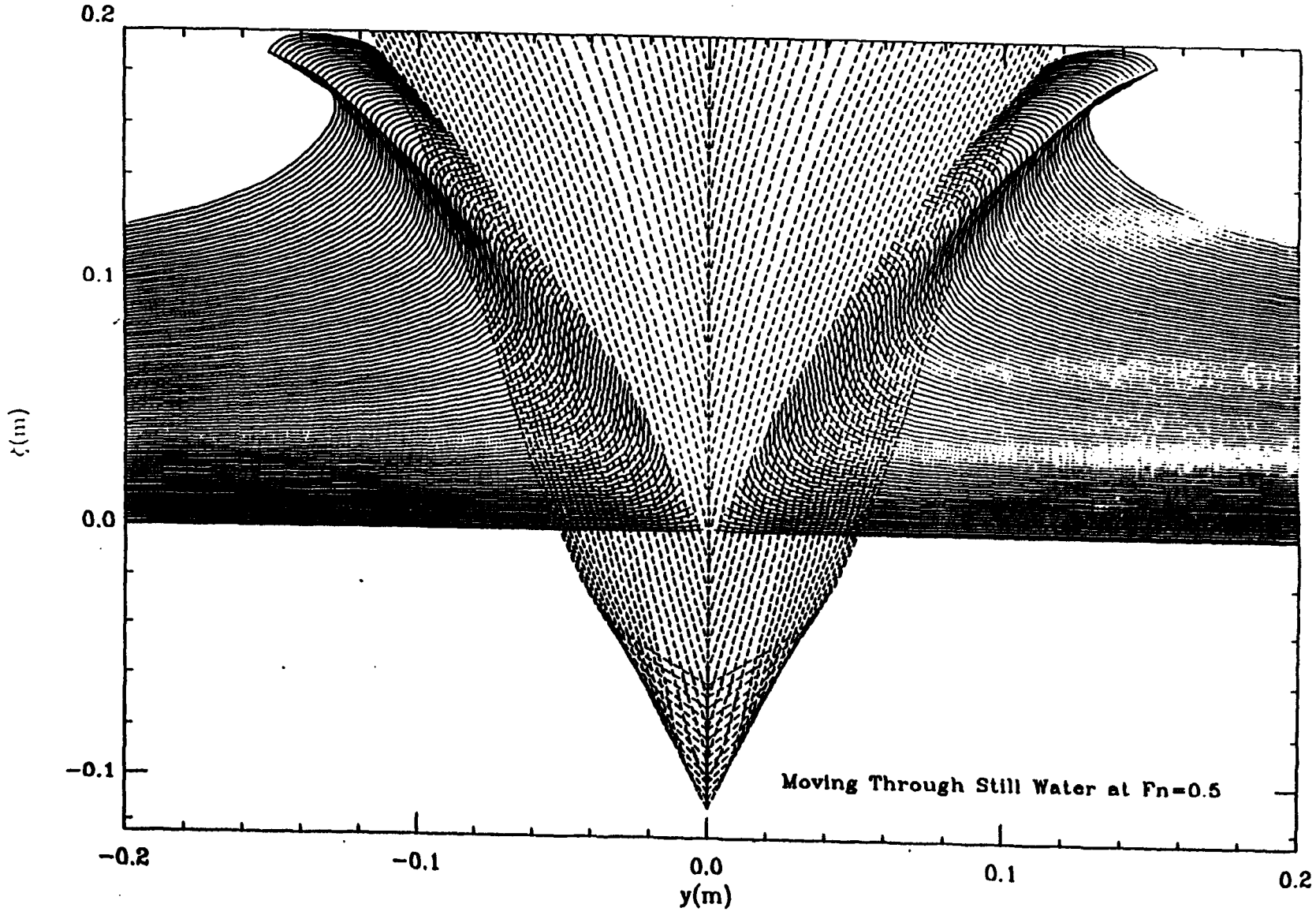
0.2
0.1
0.0
−0.1
ζ(m)
−0.2
−0.1
0.0
0.1
0.2
y(m)
Moving Through Still Water at Fn=0.5

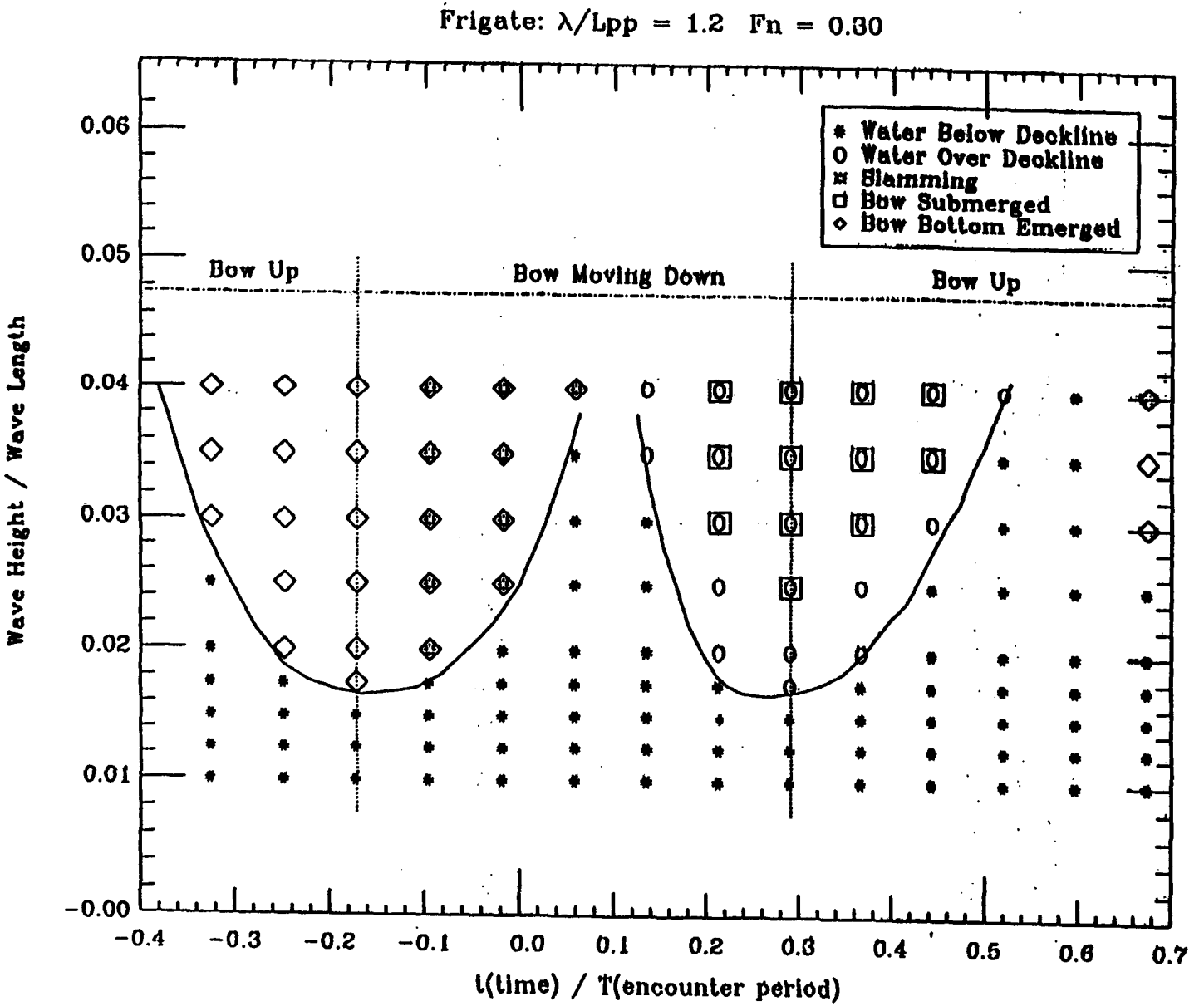

Deck Wetness, Slamming, vs. Wave Parameters

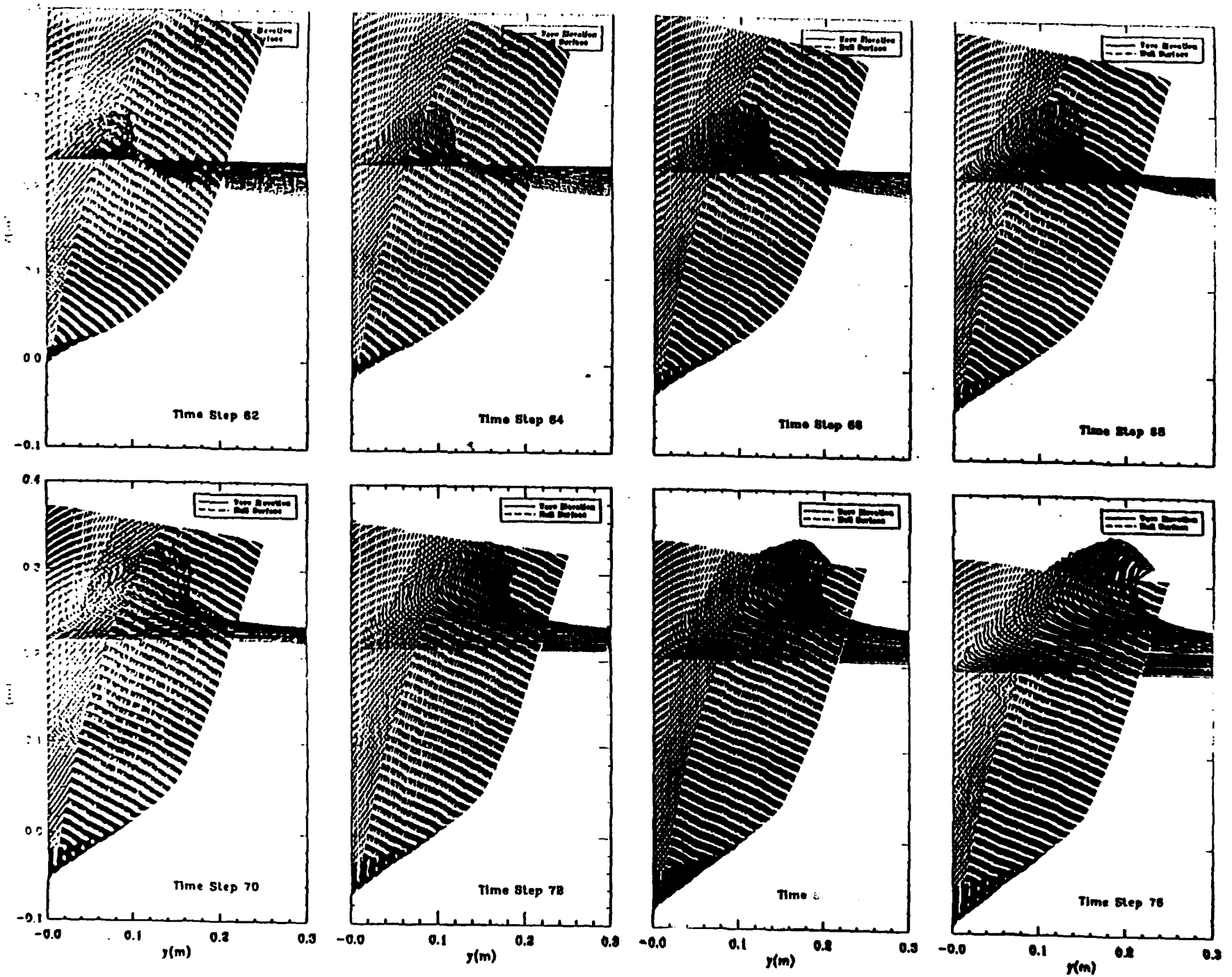

Wave Generated At Bow of a Frigate, $\lambda/Lpp=1.2$, $H/\lambda=0.025$, $Fn=0.3$

15. TULIN

Frigate: $H/\lambda = 0.025$; $Fn = 0.30$

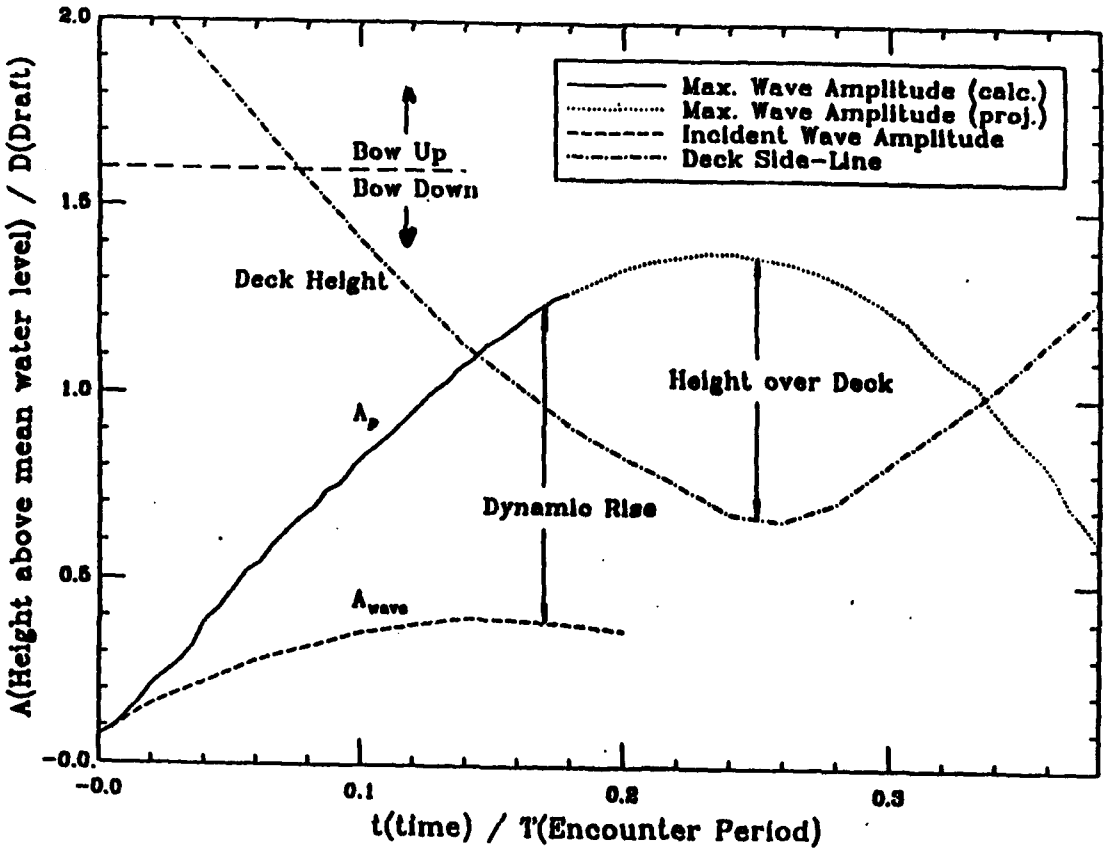

Peak water elevation, A_p, computed in time using non-linear slender body theory

Enclosure B

FINAL TECHNICAL REPORT

BY

PROF. H. MARUO AND DR. W. SONG

Nonlinear Analysis of Bow Wave Breaking and Deck Wetness

Hajime Maruo and Wusheng Song

1 Introduction

Among various problems of seakeeping qualities of ships, deck wetness or shipping of water becomes important espacially in high speed operation in rough seas. It is a governing factor for determination of freeboard and the design of flare at the bow in ship design practice. The existing method of theoretical prediction of seakeeping qualities depends on the linearized theory of the fluid motion around the hull. In practice, hydrodynamic forces on the hull are predicted by means of the strip theory. It is generally accepted that the ship motion determined from the linear equation of the motion with hydrodynamic coefficients, derived from the linearized theory in two dimensions, shows a fairly good prediction for the ship behavior among waves, unless in very severe conditions. However it is known that some of the prediction by means of the linearized theory is not necessarily satisfactory in several problems of seakeeping characteristics including deck wetness and slamming impact. Deck wetness, which is the problem of the present interest, is determined by relative height of the deck above the disturbed sea surface. The simplest approximation by the existing practice is that the wave surface is taken as if it were undisturbed by the existence of the ship hull. It is clear that this is a too coarse assumption, because elevation of the sea surface changes due the disturbance by the hull to a considerable extent, so that the interaction between the hull and the free surface should be taken into account by the prediction of free surface elevation. The heave of the sea surface due to the disturbance by the hull is called the dynamic swell. The existing practice employs the strip theory with the linearized theory in two dimensions applied to each cross section of the hull. Takaishi et al(1972) calculated the relative height of the deck above the disturbed wave surface of a container ship by the above method. Fairly good agreement was observed between computation and experiment. Since this is the case of large container ship at forward speed of moderate Froude number, the ship motion is comparatively mild, and the linearized theory seems to work well. However the condition is different when the ship is operating at high speed in rough seas. Nonlinearity becomes remarkable in the fluid motion around the hull, and breaking wave or spray is observed at the bow, which is likely to have a considerable effect on shipping water. These phenomena are quite nonlinear and there has been no reliable method so far to predict deck wetness in such a severe condition.

As the analytical solution is not applicable to the nonlinear boundary value problem, which appears in the present case, the analysis depends on the numerical method in general. Although recent development of the computational fluid dynamics enables the numerical solution of the fully three-dimensional nonlinear free surface flow problem, the three-dimensional computation in the present problem does not seem pratical because of large computer time and insufficient accuracy. The strip theory is the simplest approximation in which nonlinear effects can be considered. However the strip theory is unable to describe the effect of forward speed to the fluid motion in rational way. Application of the slender body technique to the ship moving through ambient ocean waves provides a rational approach. The existing theory of this kind is based on a series expansion of the solution with respect to two small parameters which are mutually independent. The slenderness ratio of the hull and the ratio of wave height to the ship's length are taken as the perturbation parameters in general. Then the first order solution is determined from a set of linear boundary value problems in two dimensions in the plane perpendicular to the longitudinal axis of the hull. Thus the slender ship theory formulated in this way belongs originally to the linearized approximation. An implication of the two parameter expansion is the condition that the amplitude of the vertical motin of the hull as well as the free surface elevation is small as compared with the dimension of the cross section of the hull, i.e. breadth and draft. However the motion amplitude is not necessarily small in comparison with the draft, even though the amplitude of oscillation and wave height are both small in comparison with the ship's length, which is taken as the reference length in the perturbation scheme. This contradiction is the consequence of the assumption that the slenderness ratio and the amplitude ratio are mutually independent. As a matter of fact, these parameters are of the same

order, and the separation of two variables is not applicable to the present analysis. Since the slenderness ratio and the amplitude ratio are of the same order, it is more rational that they are expressed by a common parameter. The perturbation expansion with respect to a single parameter leads to another set of boundary value problems, which is different from the existing slender ship theory based on the two parameter expansion. A great advantage of this scheme is that the first order solution allows the large amplitude motion in the local scale, even if a small amplitude is assumed in the global scale based on the ship's length. Different from the existing slender ship theory, the boundary value problem becomes nonlinear in the new approach. This may bring some complication in the solution technique. However the remarkable progress of the computational fluid dynamics in recent years has enabled the solution of fully nonlinear boundary value problem of the free surface flow to be tractable at least in two dimensions.

As far as the ship has no forward speed, the principal idea of the solution is similar to the nonlinear strip theory, by which the fluid motion at each transverse plane is purely two-dimensional and independent each other. When the finite forward speed is introduced, however, the fluid motion in a transverse plane at one cross section is subject to the effect of the fluid motion at other cross section. Then the fluid motion around the hull becomes substantially three-dimensional. A great advantage of the slender body technique is that the three-dimensional fluid motion is determined by the solution of the two-dimensional boundary value problem at each cross section even though the fluid motion is three-dimensional. Then the numerical solution for the nonlinear free surface flow is much simplified from the fully three-dimensional solution. The numerical method for the solution of fully nonlinear free surface problem in two dimensions, which has been developed recently, is available in the solution of the three-dimensional problem in this manner.

In order to examine deck wetness, one must determine

1. Vertical movement of the deck.
2. Height of the free surface at the hull surface.

The vertical movement of the deck is determined from the equation of motion of the hull. Since the fluid motion around the hull is nonlinear, the hydrodynamic forces and moments are nonlinear functions of the ship and the incident wave. According to experimental data however, the nonlinearity of the hydrodynamic forces and moments acting on the hull as a whole is not remarkable except in such extreme conditions that bottom slamming takes place. It is generally accepted that the solution of linear equations of motion predicts the ship motion fairly well, if the hydrodynamic coefficients in the equatons are suitably chosen. Correction may be applied to the hydrodynamic coefficients determined by the linear strip theory in order to illustrate the nonlinear effect. The nonlinear slender ship theory enables the nonlinear computation of hydrodynamic forces and moments. Then the ship motion may be determined by integration of the nonlinear equation of motion, but the numerical work will become enormous. In the present work, the ship motion is assumed to be given by a simple equation. Then the boundary condition on the hull surface is given by known functions, and the fluid motion around the hull is determined under given boundary conditions both on the hull surface and on the free surface.

Several problems are encountered in the development of a reliable computation scheme. The numerical solution shows instability sometimes. Another problem of difficulty is treatment of the intersection of the hull surface and the free surface, when the boundary condition takes different form on two boundaries of different kinds. Since the level of the point of intersection is the measure of deck wetness, determination of it is very important in the present problem. Wave breaking and spray are likely to appear on the bow region. The computation scheme should be able to handle the fluid motion accompanied by wave breaking and spray generation.

In the present work, effort is made to overcome the above difficulties in order to find out a method of determining the free surface elevation at the bow, which governs deck wetness, when wave breaking or spray generation is present. The aim of this work is to develop a method of predicting deck wetness, which is more accurate than the existing mothed based on the linearized strip theory.

2 Outline of the mathematical formulation

Take the cartesian coordinates x, y, z fixed in space with the origin in the still water plane, with x and $y-$axes taken horizontally and $z-$axis taken vertically upwards.

The fluid is assumed as inviscid and incompressible. Then the fluid motion started from rest is irrotational and is specified by the velocity potential Φ which satisfies the Laplace eqution in the space occupied by the fluid.

[L] $$\Phi_{xx} + \Phi_{yy} + \Phi_{zz} = 0 \tag{1}$$

where subscripts mean the partial derivatives. The boundary condition for Φ consists of two parts. One is the boundary condition on the hull surface and the other is on the free surface.

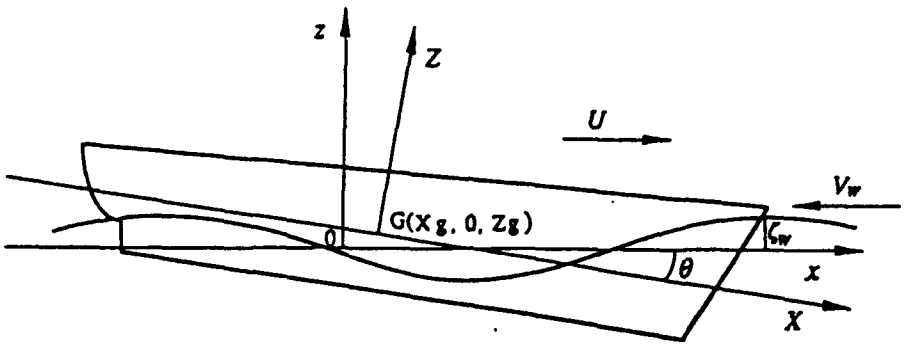

Figure 1 Coordinate system

As shown in Figure 1, consider a ship moving through a regular train of waves with average forward speed U in the direction of positive $x-$axis. Take another coordinate system (X, Y, Z) fixed to the ship. with $X-$axis along the longitudinal axis of the ship, $Y-$axis athwart ships and $Z-$axis in the upward direction. The incident wave is taken to propagate in the $x-$direction with the profile expressed by the equation

$$z = \zeta_w = A\sin(kx + \omega t + \varepsilon_0) \tag{2}$$

where $k = 2\pi/\lambda = \omega^2/g$, λ is the wave length and ω is the circular frequency. The ship makes oscillations with three degrees of freedom, i.e. surge, heave and pitch. The motion of the ship is expressed by coordinates of the center of gravity $(x_G, 0, z_G)$ in terms of the $x, y, z-$axes, and the pitching angle θ. positive in the bow down ratation.The following transformation is valid between the coordinate system (x, y, z) and (X, Y, Z).

$$\begin{aligned} X &= (x - x_G)\cos\theta - (z - z_G)\sin\theta \\ Y &= y \\ Z &= (x - x_G)\sin\theta + (z - z_G)\cos\theta \end{aligned} \tag{3}$$

The geometry of the hull surface is expressed by the equation

$$Y = F(X, Z) = f(x, z, t) \tag{4}$$

The body boundary condition at the hull surface S_H is

[H] $$f_t + \Phi_x f_x + \Phi_z f_z - \Phi_y = 0 \quad \text{on } S_H \tag{5}$$

Writing

$$F_X = \partial F/\partial X, \quad F_Z = \partial F/\partial Z$$

one can express (5) in the form

[H] $$\begin{aligned} &(-\dot{x}_G\cos\theta + \dot{z}_G\sin\theta - Z\dot{\theta})F_X + (-\dot{x}_G\sin\theta - \dot{z}_G\cos\theta + X\dot{\theta})F_Z \\ &+\Phi_x f_x + \Phi_z f_z - \Phi_y = 0 \end{aligned} \tag{6}$$

where dots mean time derivatives.

The free surface condition consists of the kinematic and the dynamic conditions. If the free surface is expressed by $z = \zeta$, the kinematic condition is

[K] $$\zeta_t + \Phi_x\zeta_x + \Phi_y\zeta_y - \Phi_z = 0 \quad \text{at } z = \zeta \tag{7}$$

The dynamic condition that the pressure is constant on the free surface is

[D]

$$\Phi_t + \frac{1}{2}\left(\Phi_x^2 + \Phi_y^2 + \Phi_z^2\right) + g\zeta = 0 \qquad \text{at } z = \zeta \tag{8}$$

The velocity potential is the sum of the incident wave potential ϕ_w and the disturbance potential ϕ, such as $\Phi = \phi_w + \phi$. We have the condition at infinity $\Phi = \phi_w$ at $\sqrt{x^2+y^2} \to \infty$. If the depth of water is infinite, we have the condition $\phi_z = 0$ at $z \to -\infty$. However these conditions for water of infinite stretch may not be convenient for numerical solution. Then the width and the depth of water are assumed finite in the actual computation.

The solution of the boundary value problem defined above is simplified to a great extent by application of the slender body theory. The fundamental assumption is that the breadth B and the draft d of the ship are both much smaller than the length L, $B/L \ll 1, d/L \ll 1$. Now let us define the slenderness ratio as $\varepsilon = d/L$, and assume $B/d = O(1)$. The slender body theory is based on a singular perturbation in the near field.

The formation is efficiently induced by the coordinate stretching technique. The governing equation is transformed to a system of stretched coordinate x', y', z' such as $x = x', y = \varepsilon y', z = \varepsilon z'$. The solution is expanded in ascending powers of ε, the governing equation is reduced to the Laplace equation in two dimensions in the transverse $y, z-$plane,

[L] $$\Phi_{yy} + \Phi_{zz} = 0 \tag{9}$$

In applying similar techniques to the boundary conditions, we assume the following,

$$\zeta/L = O(\varepsilon), \qquad z_a/L = O(\varepsilon), \qquad \theta = O(\varepsilon)$$

Then the hull surface condition is transformed to

[H] $$\frac{\partial \Phi}{\partial n} = -\left[UF_X + \left(U\theta + \dot{z}_a - \overline{X}\dot{\theta}\right)F_Z\right]\left[1 + F_Z^2\right]^{-1/2} \tag{10}$$

where n is the outward normal of the hull contour and we can put $\overline{X} = x - x_a$. The kinematic and dynamic free surface conditons become

[K] $$\zeta_t + \Phi_y\zeta_y - \Phi_z = 0 \qquad \text{at } z = \zeta \tag{11}$$

[D] $$\Phi_t + \frac{1}{2}\left(\Phi_y^2 + \Phi_z^2\right) + g\zeta = 0 \qquad \text{at } z = \zeta \tag{12}$$

In the derivation of the above equations, we have assumed $\omega_1\sqrt{d/g} = O(1)$, where ω_1 is the circular frequency of encounter, $\omega_1 = \omega + kU$, otherwise the free surface condition is a trivial.

Since the velocity potential is decomposed as

$$\Phi = \phi_w + \phi \tag{13}$$

The boundary condition for the disturbance potential ϕ becomes

[H] $$\frac{\partial \phi}{\partial n} = -\left[UF_X + \left(U\theta + \dot{z}_a - \overline{X}\dot{\theta}\right)F_Z\right]\left[1 + F_Z^2\right]^{-1/2} - \frac{\partial \phi_w}{\partial n} \tag{14}$$

If the incident wave is not steep, one can write

$$\frac{\partial \phi_w}{\partial z} = \frac{\partial \zeta_w}{\partial t} = \dot{\zeta}_w \tag{15}$$

Putting

$$V = U\theta + \dot{z}_a - \overline{X}\dot{\theta} - \dot{\zeta}_w \tag{16}$$

the hull surface condition is written as

[H] $$\frac{\partial \phi}{\partial n} = -\left(UF_X + VF_X\right)\left(1 + F_Z^2\right)^{-1/2} \qquad \text{on } \Gamma_H \tag{17}$$

The free surface elevation due to the disturbance is

$$\zeta_1 = \zeta - \zeta_w \tag{18}$$

Then the kinematic free surface condition can be written as

[K] $$\zeta_{1t} + \phi_y\zeta_{1y} - \phi_z = 0 \qquad \text{at } z = \zeta = \zeta_w + \zeta_1 \tag{19}$$

The dynamic condition becomes on the other hand

$$[D] \qquad \phi_t + \frac{1}{2}(\phi_y^2 + \phi_z^2) + \phi_z \dot{\zeta}_w + g\zeta_1 = 0 \qquad \text{at } z = \zeta_w + \zeta_1 \tag{20}$$

ζ_1 and ϕ at the free surface are determined by integration of (19) and (20) with time with a suitable initial condition. It is more convenient to employ the Lagrangean time derivative in order to integrate the above equations with time. The Lagrangean derivative or the material derivative in the two-dimensional $y, z-$plane is defined by

$$\frac{d}{dt} = \frac{\partial}{\partial t} + \phi_y \frac{\partial}{\partial y} + \phi_z \frac{\partial}{\partial z} \tag{21}$$

Then the kinematic condition is written as

$$[K] \qquad \frac{d\zeta_1}{dt} = \phi_z \qquad \text{on } z = \zeta_w + \zeta_1 \tag{22}$$

while the dynamic condition is written as

$$[D] \qquad \frac{d\phi}{dt} = \frac{1}{2}(\phi_y^2 + \phi_z^2) - \phi_z \dot{\zeta}_w - g\zeta_1 \qquad \text{at } z = \zeta_w + \zeta_1 \tag{23}$$

Thus the free surface from $z = \zeta$ and value of ϕ on the free surface are determined from (22) and (23) respectively, but we must know the values of ϕ_y and ϕ_z on the free surface before integrating the above equations. The fluid velocities ϕ_y, ϕ_z are determined by the solution of the two-dimensional Laplace equation

$$[L] \qquad \phi_{yy} + \phi_{zz} = 0 \tag{24}$$

which satisfies both the hull surface condition (17) and the free surface condition (22)(23).

It should be noted that the condtion at infinity, $\phi \to 0$ as $y \to \pm\infty$, is not applied, because the solution is valid only in the near field. The solution of (24) is generally expressed in the form $\phi_1 + g(x)$, where ϕ_1 satisfies the boundary conditon and vanishes at infinity and $g(x)$ is an arbitrary function of x only, which gives some indeterminateness to the solution. In order to make the solution definite, one has to determine $g(x)$ by matching with the far field solution which may be obtained in another way. According to the linearized slender ship theory however, it id proved that $g(x)$ becomes negligible under the condition $\omega\sqrt{d/g} = O(1)$. Therefore the condition at infinity holds in the present case.

3 Solution procedure

The slender body technique reduces the problem to the two-dimensional boundary value problem in the plane perpendicular to the longitudinal axis of the ship as explained in the previous section. One must remember that the problem is formulated in the coordinate system fixed in space rather than the coordinate system moving with the ship. Therefore the solution is found in the transverse plane fixed in space, and the hull is moving relatively to this plane as shown in Figure 2. The cross section of the hull in the plane of solution at one instant is different from the cross section in the same plane at another instant.

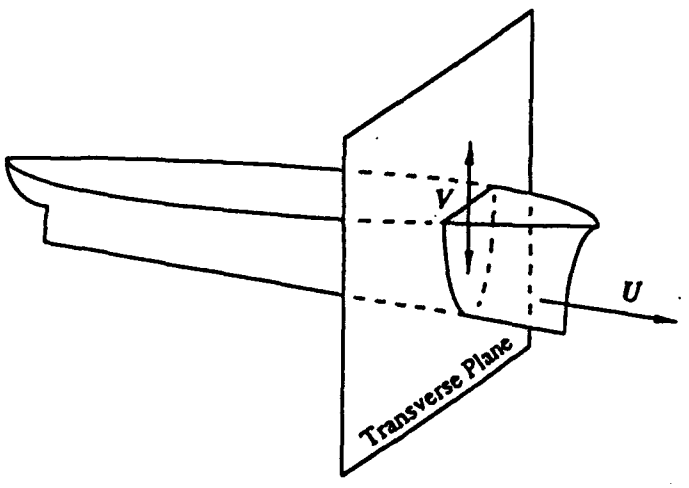

Figure 2 A transverse plane through which a ship moves

Take a transverse plane at a certain position $x = x_1$ as the plane of solution. The domain in this plane occupied by the fluid is bounded by the hull cross section Γ_H and the intersection of the free surface Γ_F. The boundary value problem is to seek the solution of the two-dimensional Laplace equation (24), which satisfies the hull surface condition (17) on Γ_H together with the free surface condition (22)(23) on Γ_F. The solution is obtained at each instant on planes at various positions $x = x_1, x_2, x_3, \cdots$. Then the three-dimensional flow field is determined.

The boundary value problem described above is solved through two steps.

[Step 1]

Assume that the value of ϕ on Γ_F is known at a certain instant $t = t_1$. The normal velocity ϕ_n on Γ_H is given by (17) if the motion of the hull is known. Now let us take a closed domain circumscribed by Γ_H, Γ_F and a contour Γ_∞ taken at a great distance surrounding the fluid domain, and apply Green's theorem in the domain Ω inside this boundary contour. Take a field point P inside Ω and a source point Q on the boundary contour $\Gamma = \Gamma_H + \Gamma_F + \Gamma_\infty$. Then Green's theorem gives

$$\phi_P = \frac{1}{4\pi}\int_\Gamma \left(\frac{\partial\phi}{\partial n} - \phi\frac{\partial}{\partial n}\right)_Q \ln\left[(y_P - y_Q)^2 + (z_P - z_Q)^2\right] ds \tag{25}$$

where n is the normal to Γ in the inward direction to Ω, and subscripts P, Q mean the values at P and Q respectively. If P is a point on Γ, the integral is taken in the sense of the Cauchy principal value, and the equation becomes

$$\phi_P = \frac{1}{2\pi}\int_\Gamma \left(\frac{\partial\phi}{\partial n} - \phi\frac{\partial}{\partial n}\right)_Q \ln\left[(y_P - y_Q)^2 + (z_P - z_Q)^2\right] ds \tag{26}$$

where $\theta = \pi$ when the contour has a continuous tangent. The normal velocity $\phi_n = \partial\phi/\partial n$ is given on Γ_H by the hull surface condition (17) while ϕ is assumed to be known on Γ_F. If the contour Γ_∞ is taken at an infinite distance, the conditon at infinity is valid and the integral along Γ_∞ has no contribution. However it is found that Γ_∞ taken at a finite distance is more conveninet for numerical solution. Here we take Γ_∞ composed of two vertial lines on both sides of the hull and a horizontal line representing the water bottom of finite depth, and impose the conditon $\phi_n = 0$ on this boundary. The value of ϕ on Γ_H and Γ_∞ is unknown, while ϕ_n on Γ_F is unknown. Then a set of simultaneous integral equations for these unknowns is derived from (26). The integral equation is solved by a numerical method.

[Step 2]

The solution of the integral equation obtained in Step 1 gives the normal velocity ϕ_n on Γ_F. Since the velocity potential ϕ is assumed to be known on Γ_F, the tangential velocity on Γ_F is obtained by differentiation of ϕ along Γ_F, $\phi_s = \partial\phi/\partial s$. The y and z components of the fluid velocity on the free surface are determined by

$$\phi_y = (\phi_s + \phi_n\zeta_{1y})/(1+\zeta_{1y}^2)^{1/2} \tag{27}$$

$$\phi_z = (\phi_s\zeta_{1y} - \phi_n)/(1+\zeta_{1y}^2)^{1/2} \tag{28}$$

The free surface elevation and the velocity potential on the free surface at subsequent instants are determined by the evolution equation (22)(23) respectively. Applying the values of (27) and (28) to (22)(23), the increment of ζ_1 and ϕ in a short interval Δt is given by

$$\Delta\zeta_1 = \Delta t\, d\zeta_1/dt \tag{29}$$

$$\Delta\phi = \Delta t\, d\phi/dt \tag{30}$$

These values are calculated with respect to a definite fluid particle. The position of the particle is determined by

$$\frac{dy}{dt} = \phi_y, \qquad \frac{dz}{dt} = \phi_z + \dot{\zeta}_w \tag{31}$$

Thus the free surface elevation $\zeta = \zeta_w + \zeta_1$ and the velocity potential on the free surface at the instant $t_2 = t_1 + \Delta t$ are determined, and the boundary value problem in Step 1 at the time $t = t_2$ is fully defined. The step by step, time marching procedure of Step 1 through Step 2 determines the evolution of the

flow field in a control plane at a definite position $x = x_1$, say. Since this is an initial value problem, the initial condition at an initial point must be defined. The initial point is at the intersection of the stem of bow with the free surface, and the computation starts at the instant when the initial point reaches the control plane. The simplest idea for the initial condition is that $\phi = 0$ on the undisturbed free surface, while the normal velocity on the hull surface is given by the hull surface condition. However it is found after some trial computation that difficulty appears in the numerical solution of Step 1 by this type of initial condition because of the singularity at the intersection of the hull surface and the free surface. The initial condition employed here is as follows. In the first time interval after the initial point, the scale of the hull cross section in the control plane is very small, that means large Froude number of local fluid motion and the effect of gravity does not contribute to the fluid motion much. If the ship has a raked stem, the motion of the hull contour in the control plane is similar to the vertical motion of a sharp wedge, for which there is an analytical solution if gravity is not present. Here we employ Mackie's (1969) solution for the entry of a sharp wedge into a free surface as the initial conditon. According to this theory, the velocity potential and the free surface elevation, when a wedge of apex angle α enters the free surface at the velocity V, are given by

$$\phi = \frac{\alpha}{2\pi} \int_0^1 \ln \frac{y^2 + (z+z')^2}{y^2 + (z-z')^2} dz' \tag{32}$$

$$z = \frac{\alpha}{\pi} \left[\ln \left(1 + \frac{1}{y^2} \right) + 2y \tan^{-1} \left(\frac{1}{y} \right) - 2 \right] \tag{33}$$

where y and z are normalized by Vt and ϕ is normalized by $V^2 t$.

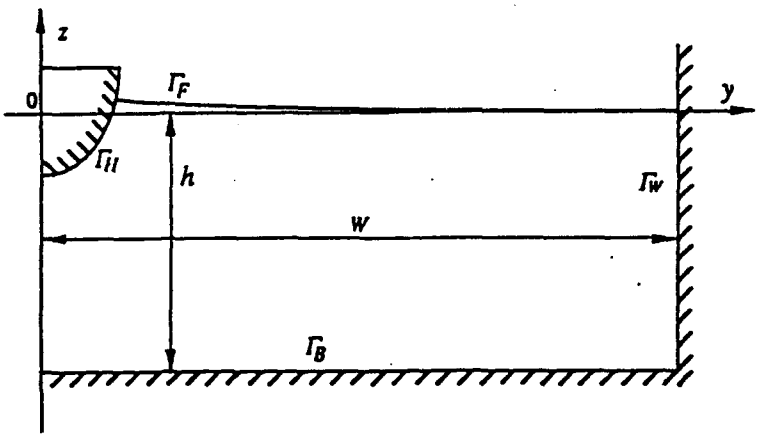

Figure 3 Computational boundary

4 Numerical method

The integral equation in Step 1 is solved by a numerical method. The boundary integral equation is written in the form

$$\theta \phi_P = \int_{\Gamma_H + \Gamma_F + \Gamma_\infty} \left(\frac{\partial \phi}{\partial n_Q} G(P,Q) - \phi \frac{\partial G(P,Q)}{\partial n_Q} \right) ds_Q \tag{34}$$

where

$$G(P,Q) = \frac{1}{2} \ln \left[(y_P - y_Q)^2 + (z_P - z_Q)^2 \right] \tag{35}$$

The numerical boundary is taken as that in Figure 3. On the hull surface contour Γ_H, ϕ_n is given by the boundary condition, and on the free surface contour Γ_F, ϕ is given by the result of computation in Step 2. On the outer boundary, we set $\phi_n = 0$. The outer boundary is divided into the side wall Γ_W and the water bottom Γ_B. The condition of the horizontal water bottom is satisfied by taking the image with respect to the bottom line at $z = -h$. Hereafter we define Γ_H and Γ_F by including their image contours.

The integral equation (34) is written for a point P on Γ_H or Γ_W in the form like

$$\theta \phi_P + \int_{\Gamma_H + \Gamma_W} \phi G_n ds - \int_{\Gamma_F} \phi_n G ds = \int_{\Gamma_H} \phi_n G ds - \int_{\Gamma_F} \phi G_n ds \tag{36}$$

where $G = G(P,Q), G_n = \partial G(P,Q)/\partial n_Q$ for brevity. If the point P is on Γ_F, the integral equation is written in the from

$$\int_{\Gamma_H+\Gamma_W} \phi G_n ds - \int_{\Gamma_F} \phi_n G ds = -\theta\phi_p + \int_{\Gamma_H} \phi_n G ds - \int_{\Gamma_F} \phi G_n ds \tag{37}$$

The right hand sides of the above equations are known quantities. The contour is divided by discrete points with small intervals by straight line segments connecting each adjacent point. The values of ϕ and ϕ_n are defined at these points, and the linear variation of ϕ and ϕ_n is assumed along each segment. The integral equation is then replaced by a set of simultaneous linear algebraic equations. The value of θ in the integral equation in this time is the angle interior to the domain Ω between each contiguous segment.

The simultaneous algebraic equations can be written in matrix form,

$$\begin{bmatrix} [A_1] & [D_1] \\ [A_2] & [D_2] \end{bmatrix} \begin{Bmatrix} \{\phi\} \\ \{\Phi\} \end{Bmatrix} = \begin{bmatrix} [B_1] & [C_1] \\ [B_2] & [C_2] \end{bmatrix} \begin{Bmatrix} \{\phi_n\} \\ \{\Phi_n\} \end{Bmatrix} \tag{38}$$

where ϕ, ϕ_n mean values on Γ_H or Γ_W, and Φ, Φ_n on Γ_F. If we write the above equation in simpler form

$$[A_{ij}]\{\phi_j\} = [B_{ij}]\{\phi_{n_j}\} \tag{39}$$

the elements of the matrices are given by

$$\begin{aligned} A_{ij} = {} & \theta_i\delta_{ij} + \frac{1}{s_j - s_{j-1}} \int_{j-1}^{j} s G_n ds - \frac{s_{j-1}}{s_j - s_{j-1}} \int_{j-1}^{j} G_n ds \\ & + \frac{s_{j+1}}{s_{j+1} - s_j} \int_{j}^{j+1} G_n ds - \frac{1}{s_{j+1} - s_j} \int_{j}^{j+1} s G_n ds \end{aligned} \tag{40}$$

$$\begin{aligned} B_{ij} = {} & \frac{1}{s_j - s_{j-1}} \int_{j-1}^{j} s G ds - \frac{s_{j-1}}{s_j - s_{j-1}} \int_{j-1}^{j} G ds \\ & + \frac{s_{j+1}}{s_{j+1} - s_j} \int_{j}^{j+1} G ds - \frac{1}{s_{j+1} - s_j} \int_{j}^{j+1} s G ds \end{aligned} \tag{41}$$

We have a system of linear algebraic equations with respect to ϕ_j on Γ_H and Γ_W and ϕ_{n_j} on Γ_F. The unknown values of ϕ on Γ_H and Γ_W and ϕ on Γ_F are determined simply by the matrix inversion using the computer. Thus the flow field in a certain transverse plane Σ at a certain instant $t = t_1$ is completely determined.

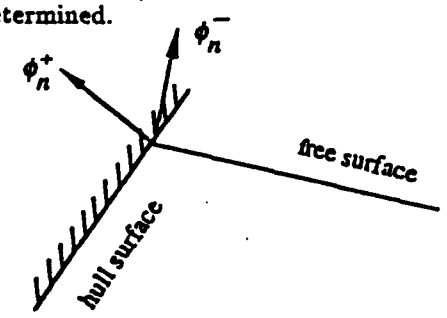

Figure 4 Intersection point

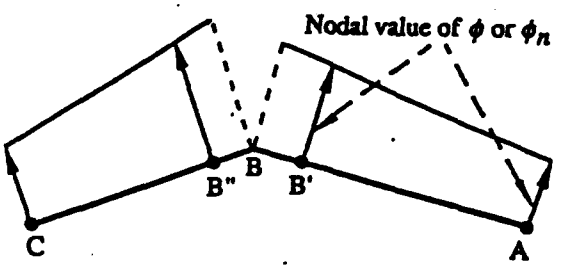

Figure 5 Discontinuous elements

There are several points which need special treatment. Since a measure of deck wetness is relative height of the wave surface at the hull surface, and the point of intersection of the hull surface and free surface presents the top of the wetted region on the hull surface, it is obvious that cautious treatment of the intersection point is very important for the prediction of deck wetness. Several researchers have presented methods to treat this point, but some of their methods seem to be inaccurate, and some are not suitable in the present problem. The values of ϕ and ϕ_n are defined at nodal points connecting adjacent line segments which replace the boundary contour. Though the potential is unique at any nodal point, the normal velocity ϕ_n does not have a unique value at nodes where the normal to the boundary is not unique. In particular, the intersection point is a special node at which ϕ is continuous while ϕ_n is different on each side because of different boundary conditions as shown in Figure 4. Write ϕ_n^+ for

the normal velocity to the hull surface and ϕ_n^- to the free surface at the intersection point. Since ϕ_n^+ is known and ϕ_n^- unknown, (39) can be transformed to

$$[A_{ij}]\{\phi_j\} = [B_{ij}]\{\phi_{n_j}\} + [C_i]\{\phi_n\} \tag{42}$$

where $\phi_n^- \in \phi_{n_j}$.

The unknown ϕ_n^- is determined from the above equation. Another kind of nodal point which needs special treatment is the tip of the spray jet which sometimes occurs. The potential is given at this point, while the unknown normal velocity at the free surface has different values on both sides of the jet. Two unknowns at the same nodal point require another equation. The method to solve this problem involves discontinuous elements introduced by Brebbia and Dominguez (1989) as shown in Figure 5. Instead of the nodal point B connecting segments AB and BC, we take a point B' on AB and B'' on BC. Then ϕ and ϕ_n are calculated at B' and B''. The values of ϕ_n at B on both sides of the jet are obtained by extrapolation.

The next time step is the determination of the free surface at the instant slightly later by a short time interval Δt. For each time step, the main computations described below are performed for the deformation of the free surface.

1) **Determination of unknowns ϕ, Φ_n :** Equation (42) is rearranged in the form

$$[A]\{X\} = \{Y\} \tag{43}$$

$$[A] = \begin{bmatrix} [A_1] & -[C_1] \\ [A_2] & -[C_2] \end{bmatrix} \tag{44}$$

$$\{X\} = \begin{Bmatrix} \{\phi\} \\ \{\Phi_n\} \end{Bmatrix} \tag{45}$$

$$\{Y\} = \begin{bmatrix} [B_1] & -[D_1] \\ [B_2] & -[D_2] \end{bmatrix} \begin{Bmatrix} \{\phi_n\} \\ \{\Phi\} \end{Bmatrix} + \begin{bmatrix} [F_1] \\ [F_2] \end{bmatrix} \{\phi_n^+\} \tag{46}$$

where $[F_1]$ and $[F_2]$ are subvectors of $[C_i]$ in (42). The right hand side of (43) is a known vector, and $\{X\}$ is determined by the matrix inversion.

2) **Time-stepping :** The position of fluid particles and values of potential ϕ, on the free surface for the next time at $t = t_1 + \Delta t$, are determined by

$$y(t_1+\Delta t) = y(t_1) + \phi_y(t_1)\Delta t \tag{47}$$

$$z(t_1+\Delta t) = z(t_1) + \phi_z(t_1)\Delta t + \zeta_w(t_1+\Delta t) - \zeta_w(t_1) \tag{48}$$

$$\phi(t_1+\Delta t) = \phi(t_1) + \left[\frac{1}{2}(\phi_n^2 + \phi_s^2) - \phi_z\dot{\zeta}_w - g\zeta_1\right]_{t_1}\Delta t \tag{49}$$

The fluid velocity ϕ_y, ϕ_z is calculated by (27) (28), and the tangential velocity ϕ_s is expressed by a finite difference of ϕ using the three point Lagrange interpolation.

3) **Smoothing :** To depress a sawtooth instability of the wave profile, the five-point smoothing algorithem is used to filter the points which are not equally spaced on the free surface. s_i in the following formula is the distance between two nodal points.

For the first point (edge point) :

$$\overline{f_0} = \frac{1}{2}\left\{\frac{1}{m-s_1}[m(f_0+f_1) - s_1(f_0+f_3)] + \frac{s_1 m}{n\ell(n-\ell)}[n(f_0-f_2) - \ell(f_0-f_4)]\right\} \tag{50}$$

For the second point :

$$\overline{f_0} = \frac{1}{2(m-s_1)}\left\{\frac{m}{s_{-1}+s_1}[s_1(f_0+f_{-1}) + s_{-1}(f_0+f_1)] - \frac{s_1}{s_{-1}+m}[m(f_0+f_{-1}) + s_{-1}(f_0+f_3)]\right\} \tag{51}$$

For the center point :

$$\overline{f_0} = \frac{1}{2}\left\{\frac{1}{s_{-1}+s_1}[s_1(f_0+f_{-1})+s_{-1}(f_0+f_1)]+\right.$$
$$\left.\frac{s_{-1}s_1}{\ell_{-2}\ell_2(\ell_{-2}+\ell_2)}[\ell_2(f_0-f_{-2})+\ell_{-2}(f_0-f_2)]\right\} \quad (52)$$

where $\ell_{-2} = s_{-2}+s_{-1}, \ell = \ell_2 = s_1+s_2, m = s_1+s_2+s_3, n = s_1+s_2+s_3+s_4$.

4) **Regridding** : In some cases, node points on the free surface, especially near the hull, are either too close to or too far from each other, leading to numerical difficulties. The regridding technique is a useful way to keep the computation accurate. If the computed distance is less than d_{min} or greater than d_{max} which are the input control parameters, the points only near the hull are redistributed by cubic spline or linear interpolation.

Thus the computation at the next time step is repeated by the above procedure 1) through 4). Since the ship is moving with forward speed U, the hull section moves astern in each time interval, and reaches the stern at the time L/U after the beginning of the above procedure at the bow. Therefore the result of computation in one round dose not express the time evolution of the free surface at a definite section of the ship nor the free surface elevation in different sections at the same instant. In order to complete the computation to obtain the result for every section throughout the length of the ship, the same computation procedures starting from the bow should be repeated by shifting the initial instant by the time interval $\Delta t = \Delta x/U$, where Δx is the interval of the section for which the result is required.

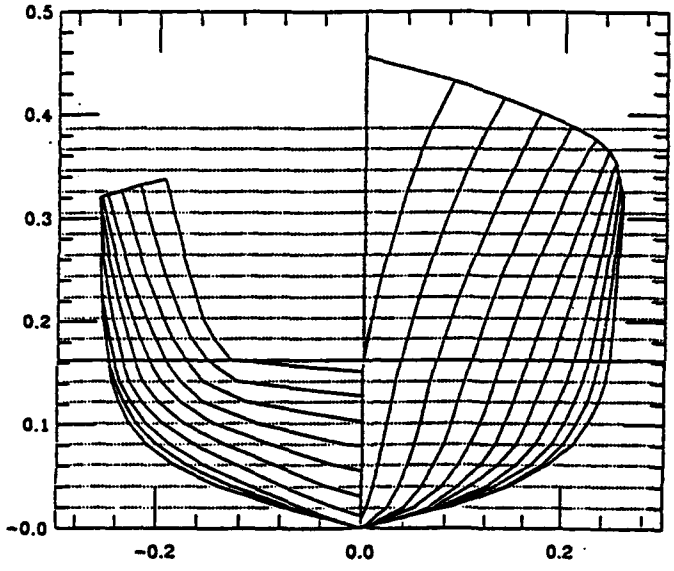

Figure 6 Body plan (L=4.5m,B=0.496m,d=0.163m)

5 Numerical Examples

A frigate model shown in Figure 6 is employed for the numerical example. The computation of ship motion in regular waves by means of the strip method and results of towing tank experiment of this model have been published by O'dea and Walden(1984).

Numerical computations are carried out in two conditions. The first is the steady forward motion in still water. The Froude number varies from 0.10 to 0.60. We take $W = 60B$ and $h = 1.2L$ as the computational domain. The number and intervals of the nodal points distributed on three boundaries Γ_H, Γ_W and Γ_F are as follows.

(1) On Γ_H : The number of nodes depends on the wetted depth of the hull contour, such as $\Delta s = d/20$ near the keel and $\Delta s = d/40$ near the point of intersection with Γ_F.

(2) On Γ_W : 15 points are distributed with an equal interval.

(3) On Γ_F : 150 points are distributed from the intersection with Γ_H in an equal interval $\Delta s = B/100$, and other 50 points are distributed along the remaining part of the boundary with arithmetic intervals.

The numerical results at the time interval Δt give the free surface profile in the transverse sections with intervals $\Delta x = U\Delta t$. The time step is chosen in such a way that the numerical results are obtained at the hull sections with the interval $\Delta x = L/800$. The reliability of the numerial results is comfirmed by changing the interval Δx and the grid density on the free surface.

The results of computation are illustrated in Figure 7 through Figure 13. At low Froude numbers less than 0.2, generation of spray is not observed, but diverging waves generated at the bow are gradually steepened and eventually break at the pointed crest, suggesting the white cap. At Froude number 0.2, overturning of the wave crest is observed, but the spray is not developed yet. At Froude number 0.3, generation of spray by the overturning free surface is clearly observed. At Froude number 0.4, some instability appears on the free surface underneath the spray root, which may suggest the spilling type of wave breaking instead of the plunging type. At Froude number 0.5, some undulation appears on the free surface under the spray sheet, and this undulation grows up further at Froude number 0.6. This phenomenon suggests another type of wave breaking.

The second case is the same ship making heaving and pitching oscillation in sinusoidal head sea waves as expressed by eq.(2) at uniform forward speed of Froude number 0.3. The length of the incident wave is so chosen as $\lambda/L = 1.2$, at which the maximum amplitude of the oscillations is observed in experiment. The ship motion is given by

$$Z = Z_A \sin(\omega_1 t + kx_G + \varepsilon_0 + \varepsilon_1)$$
$$\theta = \theta_A \sin(\omega_1 t + kx_G + \varepsilon_0 + \varepsilon_2)$$

where $\omega_1 = \omega + kU$ and x_G is the $x-$coordinate of the center of gravity referred to the origin at F.P.. Values of Z_A, θ_A, ε_1 and ε_2 are taken from experimental data of O'dea et al.

The position of the control plane is defined by the phase angle of the incident wave on the control plane at the instant when the foremost point of the bow arrives at this control plane as shown in Figure 14, and the numerical procedure starts at this instant. If the control plane fixed in space is arranged with the interval Δx_0, the phase difference between adjacent planes is $\Delta\varepsilon_0 = (\omega_1/U)\Delta x_0$. The numerical results for the free surface profile are obtained at hull sections with the interval $\Delta x = L/1000$, so the time interval of the computation is chosen as $\Delta t = 0.002256$ seconds. The reliability of the numerical results is checked by changing the interval Δx and the grid density as before.

Three kinds of the wave steepness (the ratio of wave height to wave length) i.e. $H/\lambda = 0.02$, 0.03 and 0.04 are chosen for the numerical examples. Computations are carried out at control planes at $\varepsilon_0 = 0.0$, $\pi/4$, $\pi/2$, $3\pi/4$, π and $7\pi/4$. However the preliminary computation has shown that there is no possibility of deck wetness at ε_0 greater than $\pi/2$, so that results with $\varepsilon_0 = 0.0$, $\pi/4$ and $\pi/2$ will given here.

1) Results of H/λ =0.02

The evolution of the free surface profile in the bow region at the control plane $\varepsilon_0 = 0.0$ is shown in Figure 15. At Section 133($X/L = -0.058$) of the hull, the level of the free surface exceeds the deck height, but water is pushed aside by the hull at the deck side. The overturning of the free surface results the sheet of spray jet directed outward, so that there is no shipping water on board as far as the vertical movement of the free surface relative to the deck is upward. At Section 201($X/L = -0.126$) however, the relative motion of the free surface turns to downward. Then water once lifted above the deck level is scooped up at the deck side, and a small amount of shipping water enters on deck as shown in Figure 16.

The result at the control plane $\varepsilon_0 = \pi/4$ is shown in Figure 17. The overturning free surface and the outward spray sheet are similar to the former case, but shipping water resulted by the relative movement of the free surface as shown in Figure 16 in the former case does not take place in this case. Another difference is the appearance of undulation of the free surface beneath the spray sheet, which may cause the breaking of free surface behind this position.

The result at the control plane $\varepsilon_0 = \pi/2$ is shown in Figure 18. The behavior of the free surface is different from the former cases. As the heave of free surface exceeds the deck level at Section 58 much closer to the stem than in the former cases due to deep immergence of the bow, the spray appears at the tip of heaved water and turns inward over the deck due to outward movement of the deck side. Then shipping water on board is resulted.

Computations at the control plane $\varepsilon_0 = 3\pi/4$, π and $7\pi/4$ show no shipping water. As a consequence, one can conclude that deck wetness begins to take place in the wave height $H/\lambda = 0.02$ at $\varepsilon_0 = 0.0$ and $\pi/2$. This result is in agreement with experimental data.

2) Results of H/λ =0.03

The behavior of the free surface is quite different from the former case, because of the greater motion of the hull. Heavy deck wetness is reported in experiment. The numerical result at $\varepsilon_0 = 0.0$ is shown in Figure 19. As the bow plunges into the wave surface, a mass of water is raised up on both sides of the deck in thick spray like liquid walls. Water at the top of the wall spreads in both directions, forming spray sheets directing inward and outward to the hull. The inward spray falls on deck, resulting heavy deck wetness. This phenomenon is similar to the collapse of a liquid column.

The result at $\varepsilon_0 = \pi/4$ is shown in Figure 20. After the heaving free surface exceeds the deck side, spray directing inward similar to the case of Figure 18 appears at the tip, bringing shipping water. A similar behavior of the free surface is observed at the hull section closer to the stem at $\varepsilon_0 = \pi/2$ as shown in Figure 21.

According to the experimental observation, the bow of the ship is lifted above the wave surface almost clear of water at the phase angle greater than $\varepsilon_0 = \pi/2$. Then slamming is likely to take place at the bow region. The present computation scheme is not application to this situation.

3) Results of H/λ =0.04

The result at $\varepsilon_0 = 0.0$ is shown in Figure 22. The free surface phenomenon like the collapse of a liquid column is similar to that in Figure 19, but in a much exaggerated form. The spray sheet at the top of lifted water is stronger, resulting heavy deck wetness.

Figure 23 shows the result at $\varepsilon_0 = \pi/4$. The heaved free surface turns inboard as exceeding the deck side and brings heavy shipping water in the bow region.

A similar phenomenon appears at the hull section closer to the stem at $\varepsilon_0 = \pi/2$ as shown in Figure 24.

6 Conclusions

Nonlinear computations of the free surface elevation at the bow region of a frigate model in the steady forward motion as well as in the heaving and pitching oscillations are carried out under the slender body approximation.

The computation for the steady forward motion well simulates the generation of spray and the breaking of bow waves. It is found that the pattern of breaking wave changes according to increase of forward speed.

The computation for the oscillating ship at forward speed of Froude number 0.30 shows the effect of the incident wave height. At the wave height of $H/\lambda = 0.02$, a mass of water is raised above the deck and pushed aside forming spray like the plunging breaker. However only a small amount of shipping water is observed. At greater wave height $H/\lambda = 0.03$ and 0.04, heavy deck wetness is resulted by falling water from the thick spray sheet at the lifted free surface over the deck. Deck wetness begins at the wave height $H/\lambda = 0.02$, and the result is in good agreement with the experimental observation.

References:

Brebbia, CA and Dominguez, J (1989). "Boundary Elements, An Introductory Course", *Computational Mechanics Publications, McGraw-Hill Company*, pp 70-74.

Mackie, AG (1969). "The Water Entry Problem", *The Quarterly Journal of Mechanics and Applied Mathematics*, Vol 22, Part 1, February 1969.

O'dea, JF and Walden, DA (1984). "The Effect of Bow Shape and Nonlinearities on the Prediction of Large Amplitude Motions and Deck Wetness", *15th Symposium on Naval Hydrodynamics, Hamburg, Germany.*

Takaishi, Y, Ganno, M, Yoshino, T, Matsumoto, N and Saruta, T (1972). "On the Relative Wave Elevations at the Ship's Side in Oblique Seas", *Journal of Society Naval Architects of Japan*, Vol 132, pp 147-158.

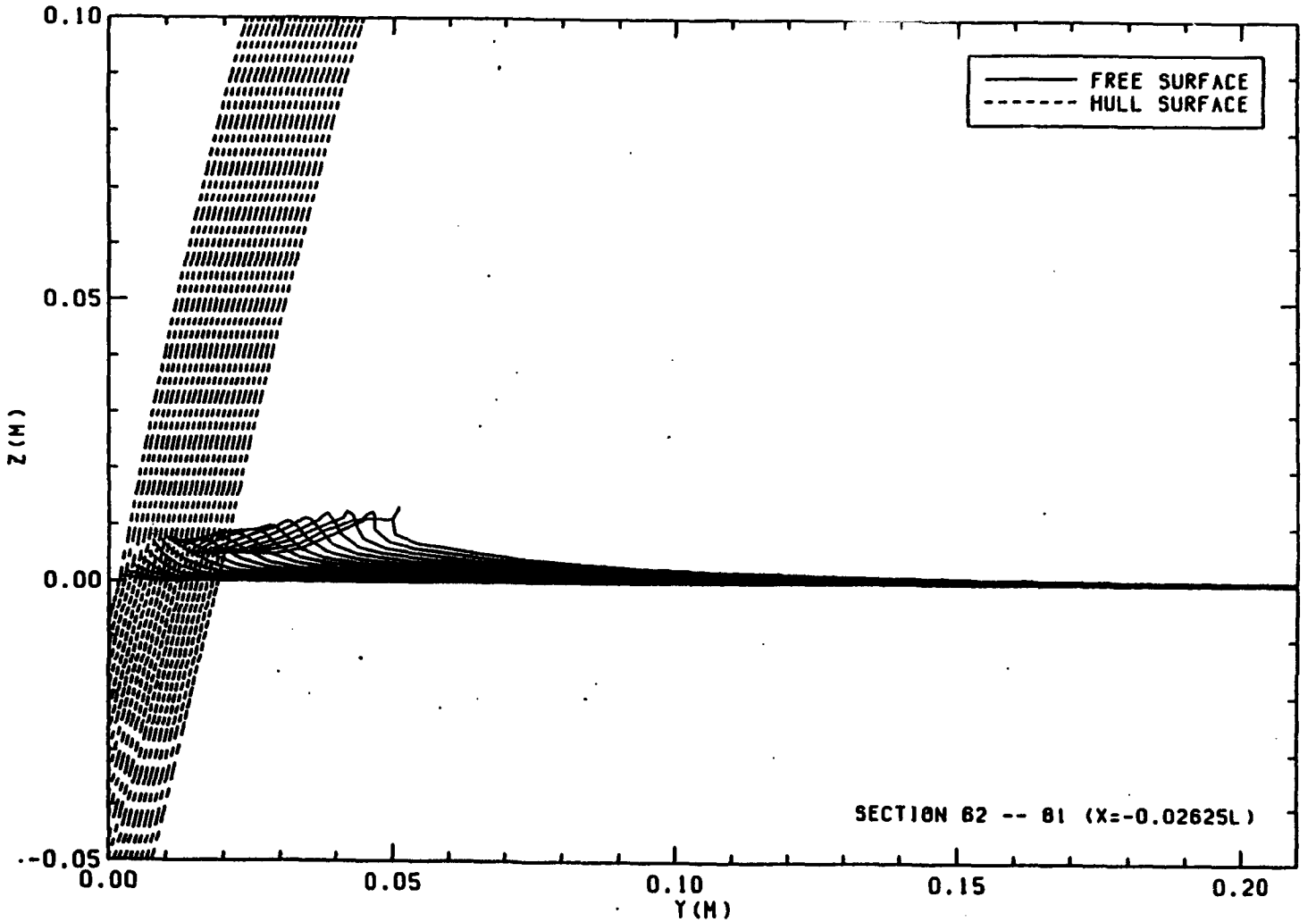

Figure 7 Bow wave breaking for a fixed ship in still water at Fn=0.10

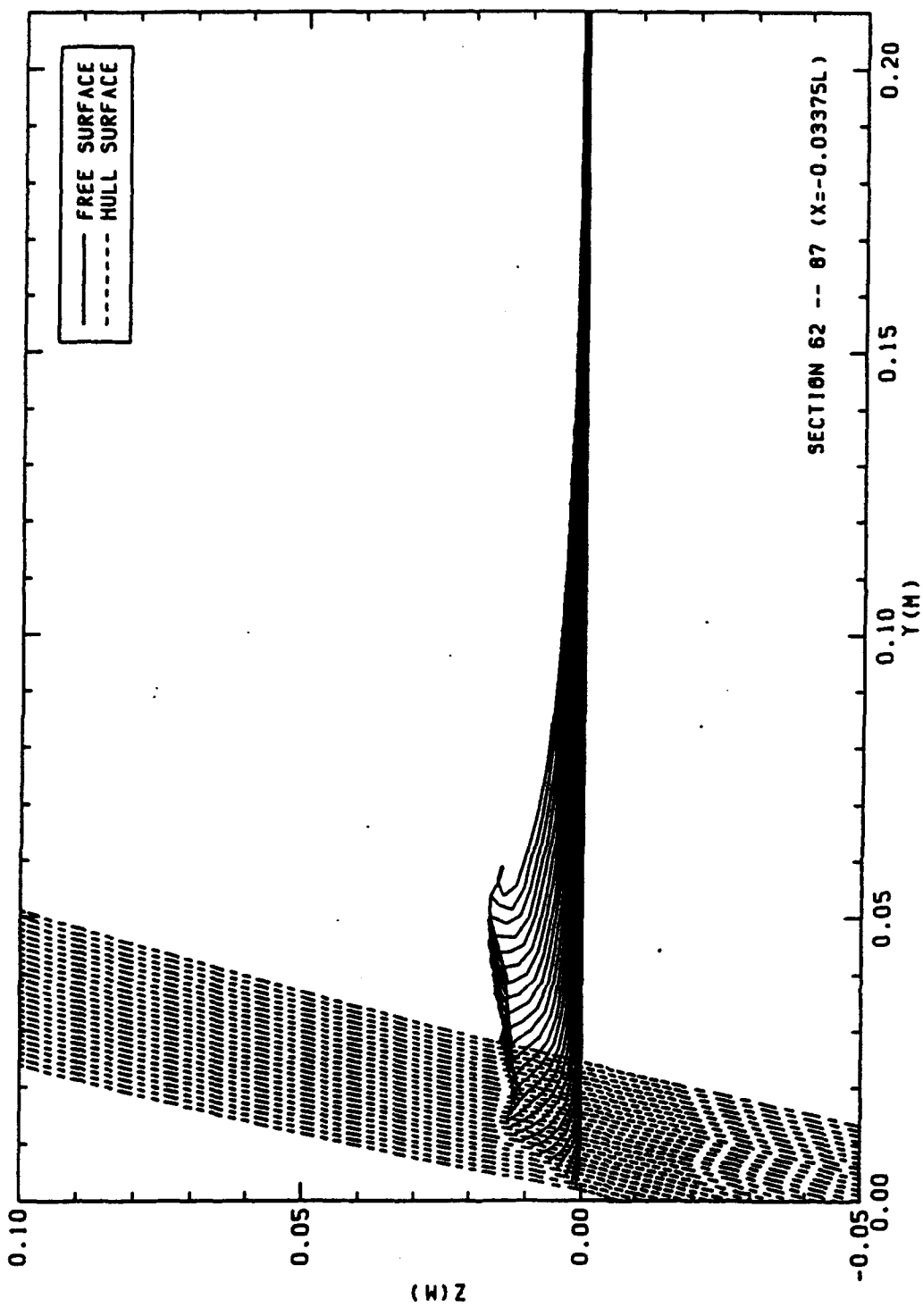

Figure 8 Bow wave breaking for a fixed ship in still water at Fn=0.15

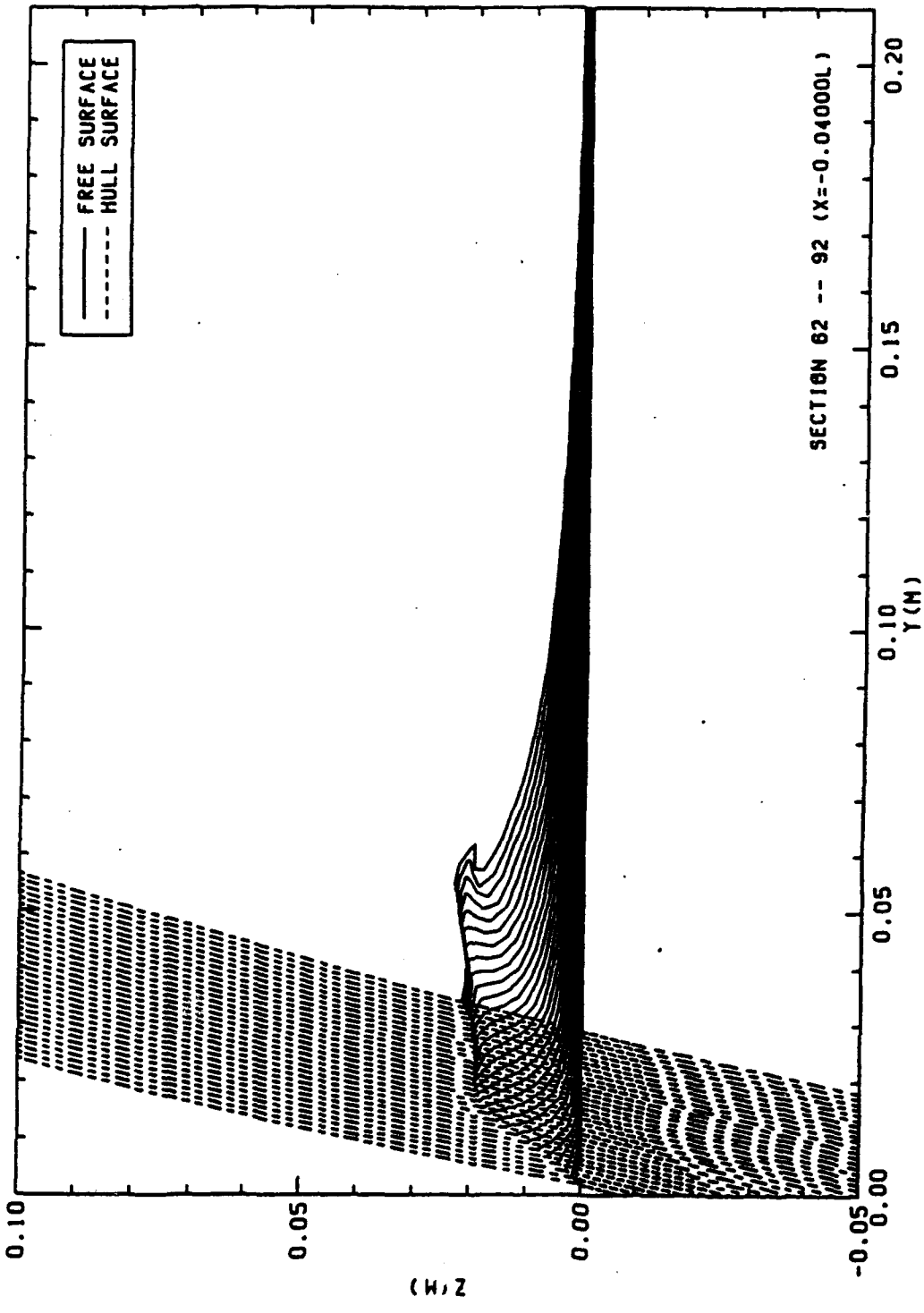

Figure 9 Bow wave breaking for a fixed ship in still water at F_n=0.20

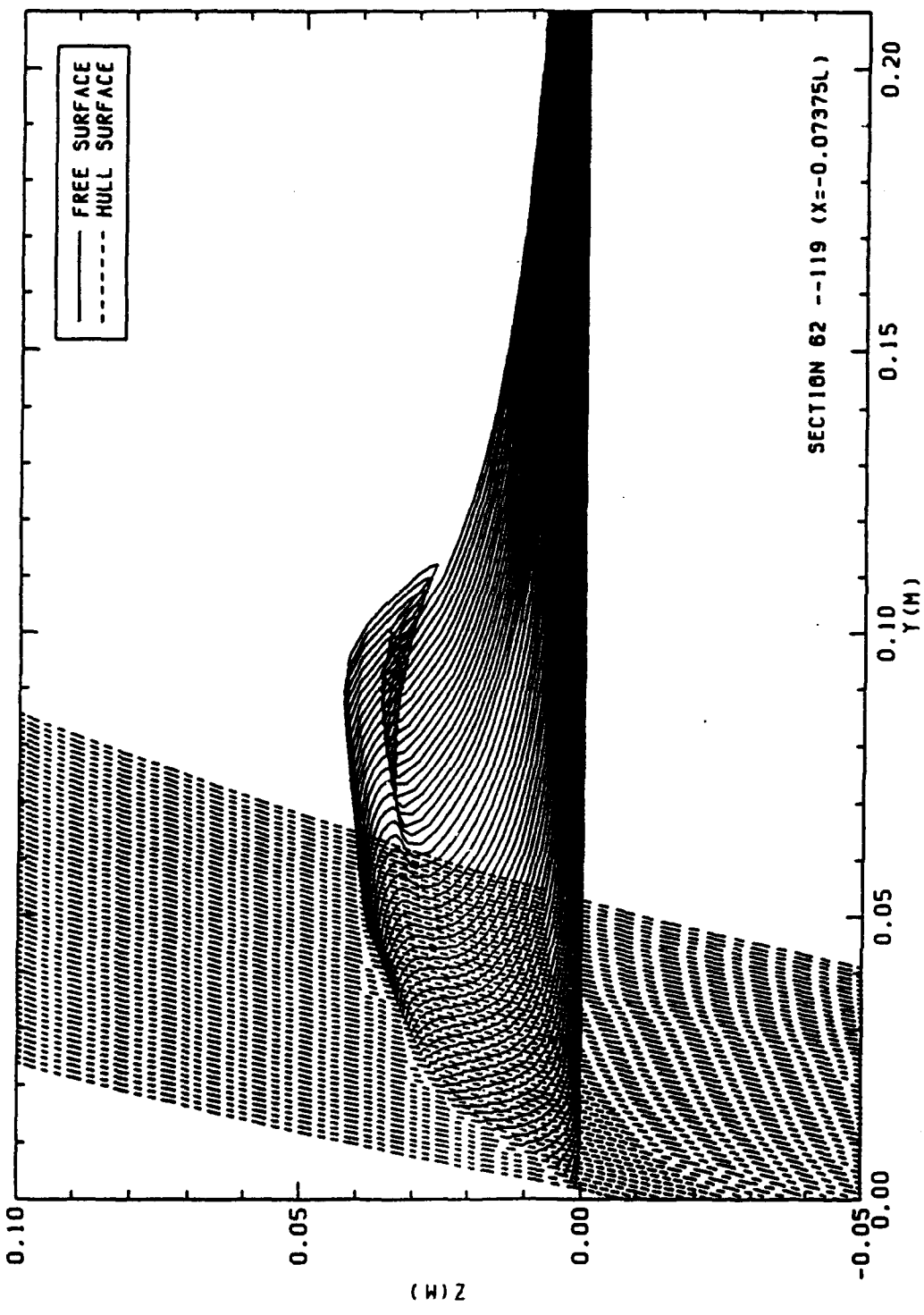

Figure 10 Bow wave breaking for a fixed ship in still water at Fn=0.30

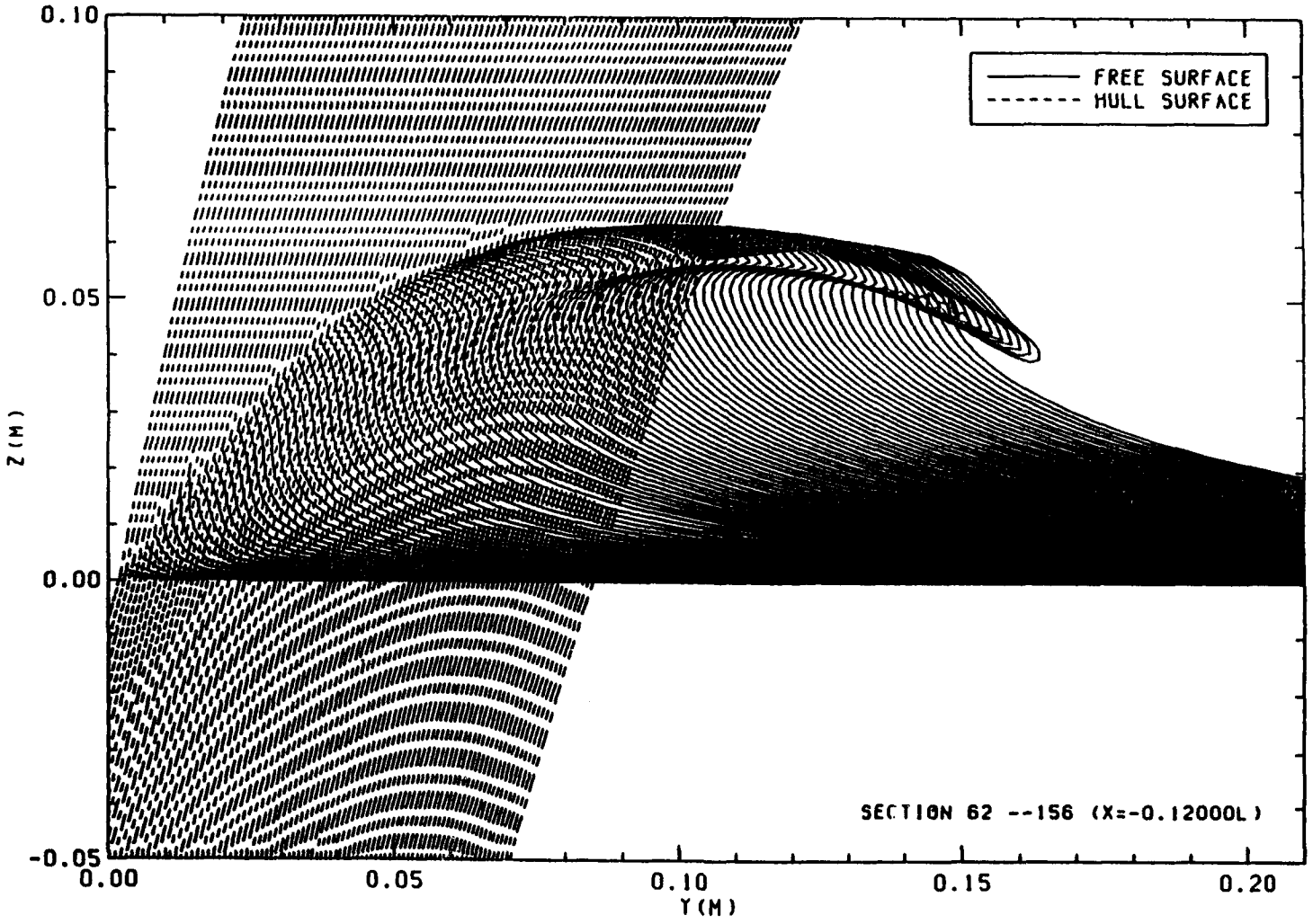

Figure 11 Bow wave breaking for a fixed ship in still water at Fn=0.40

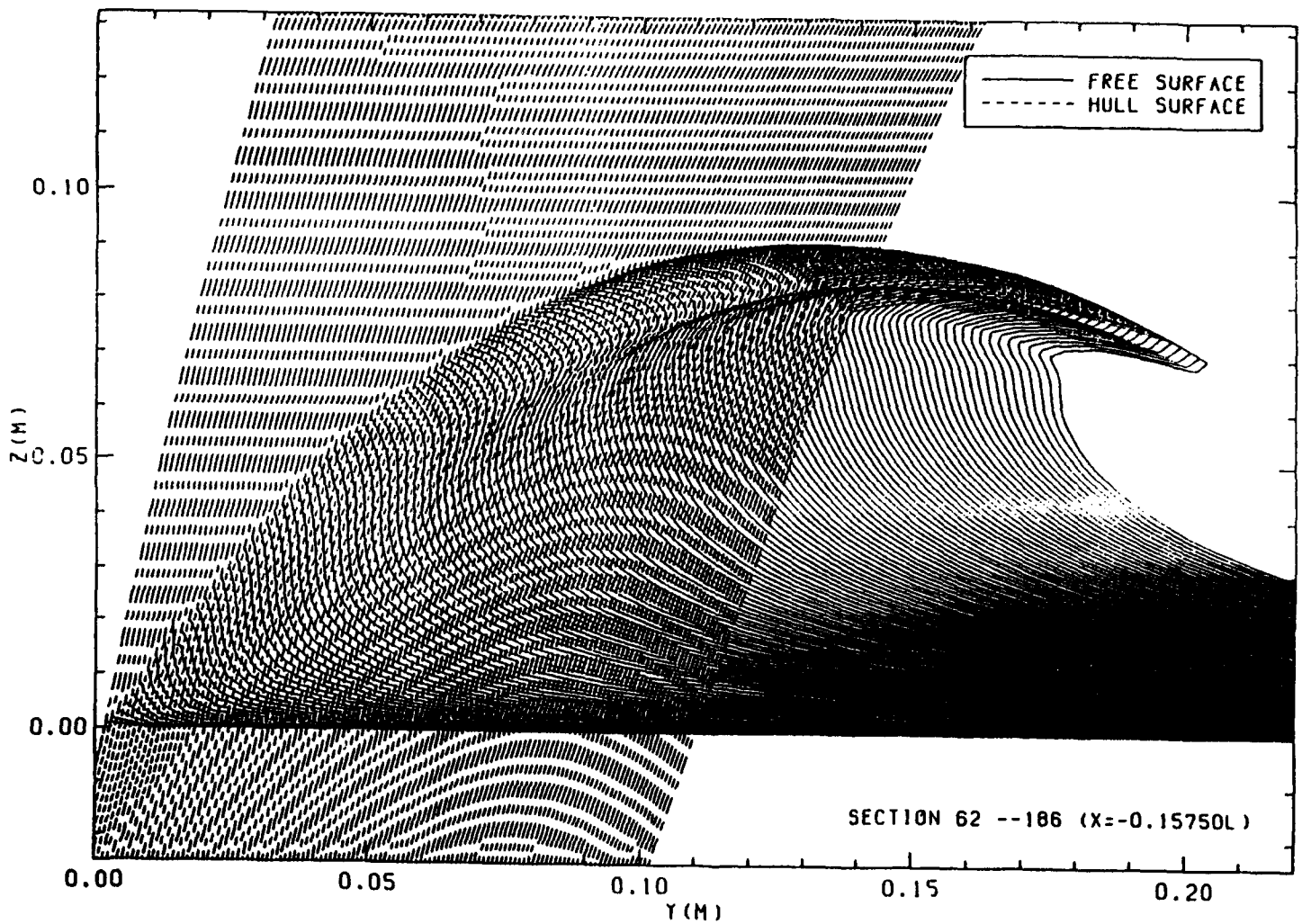

Figure 12 Bow wave breaking for a fixed ship in still water at Fn=0.50

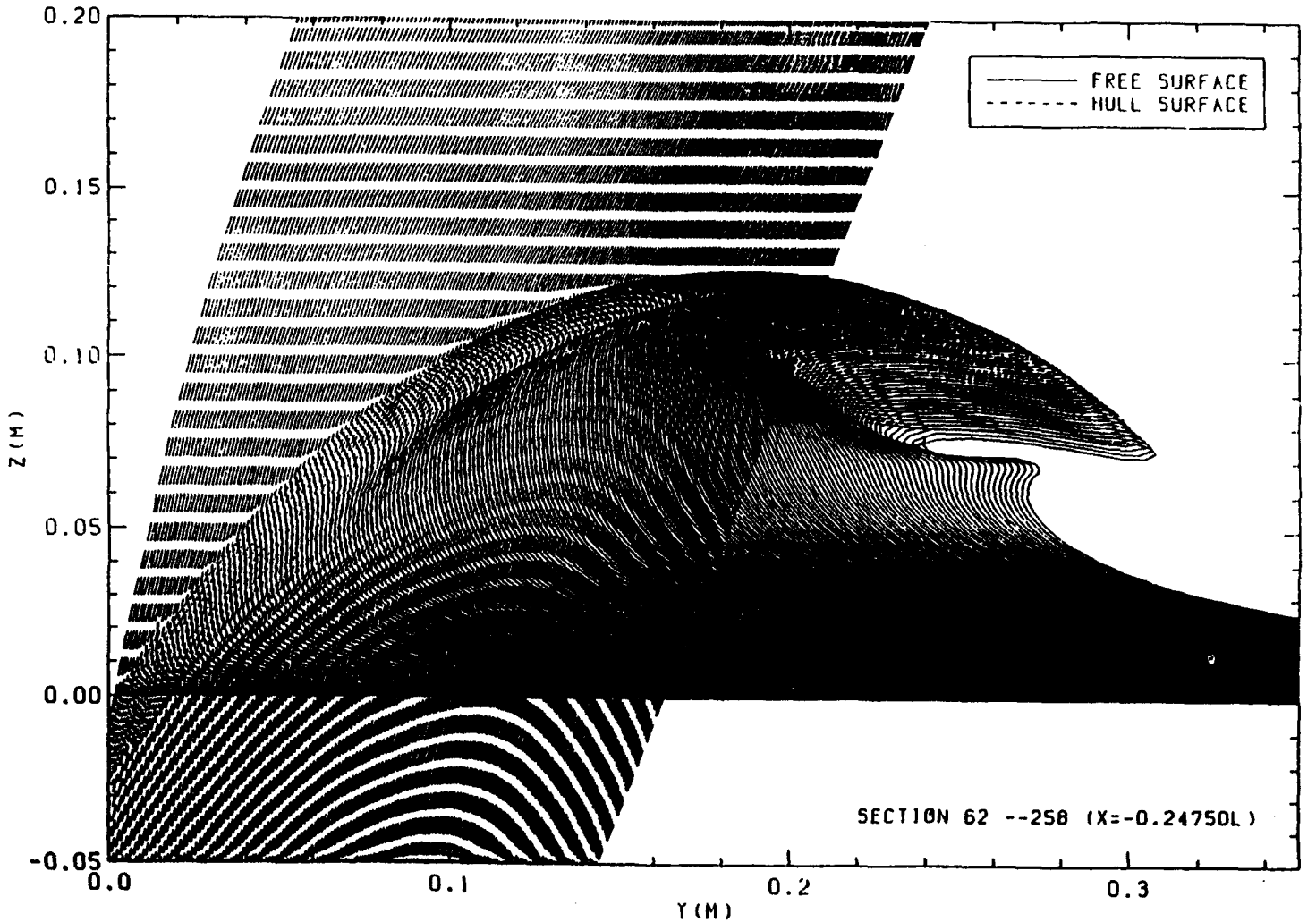

Figure 13 Bow wave breaking for a fixed ship in still water at Fn=0.60

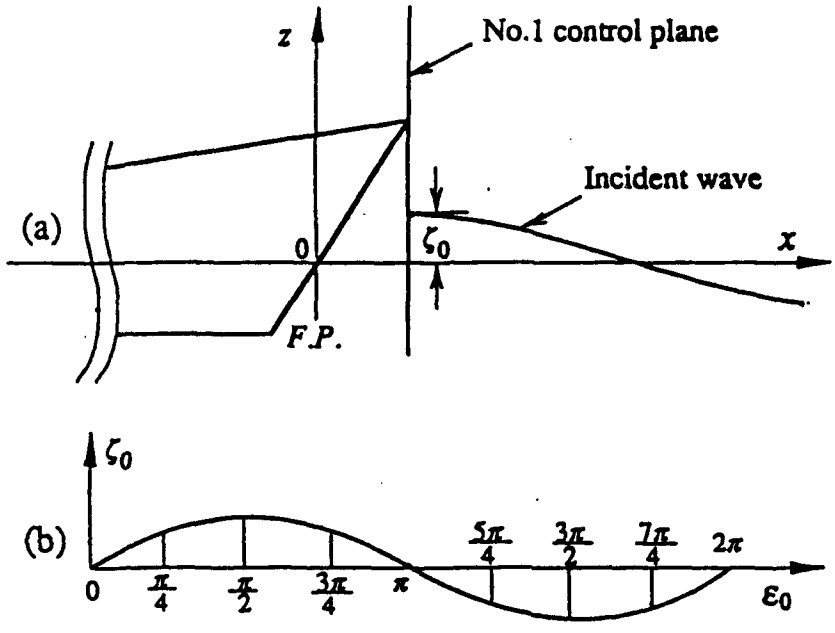

Figure 14 The position of the No.1 control plane (a) and the expresstion of the initial phase of wave (b)

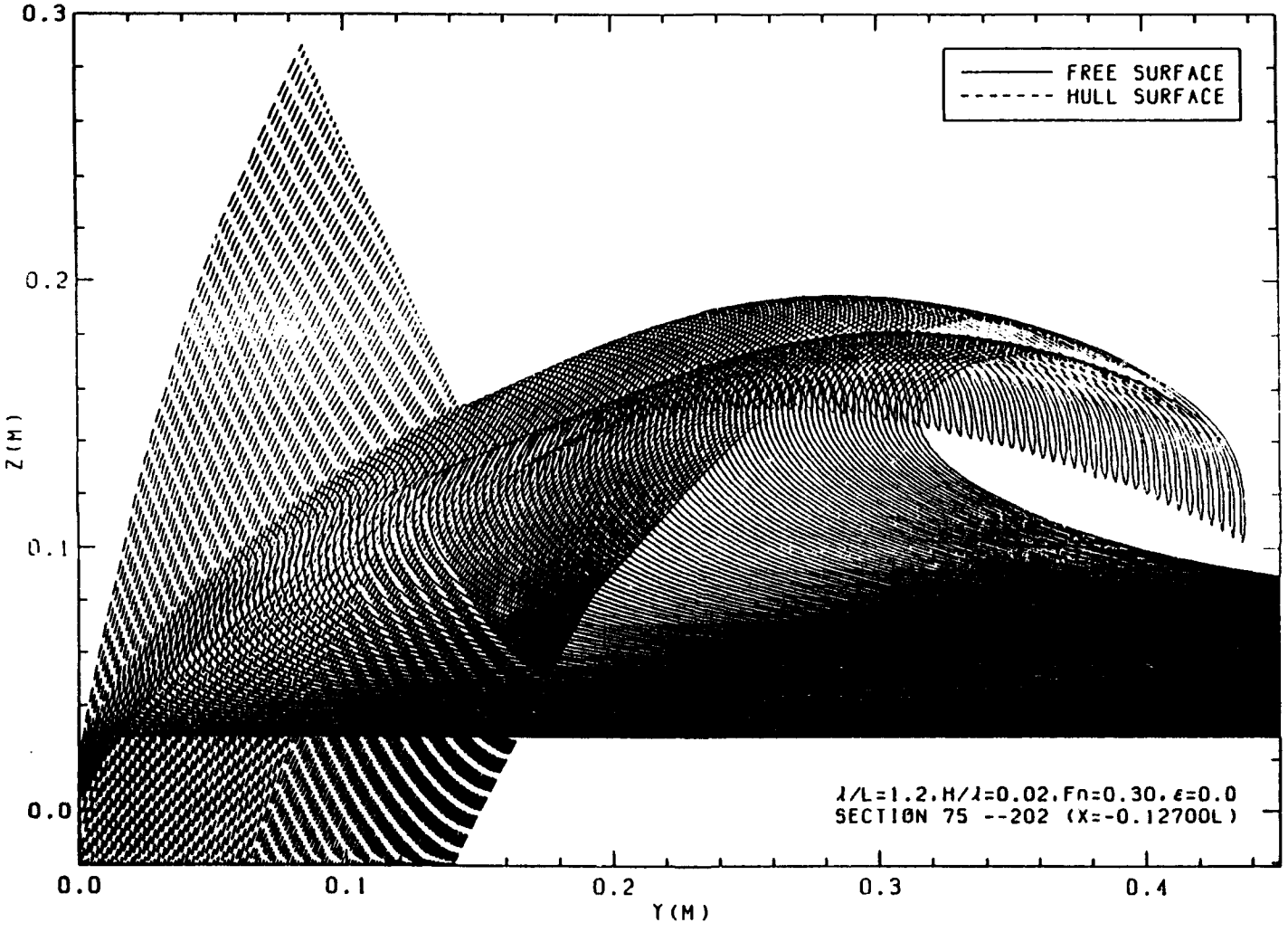

Figure 15 Wave elevation for a ship making heaving and pitching oscillation in sinusoidal head sea waves with H/λ=0.02 and ε=0.0

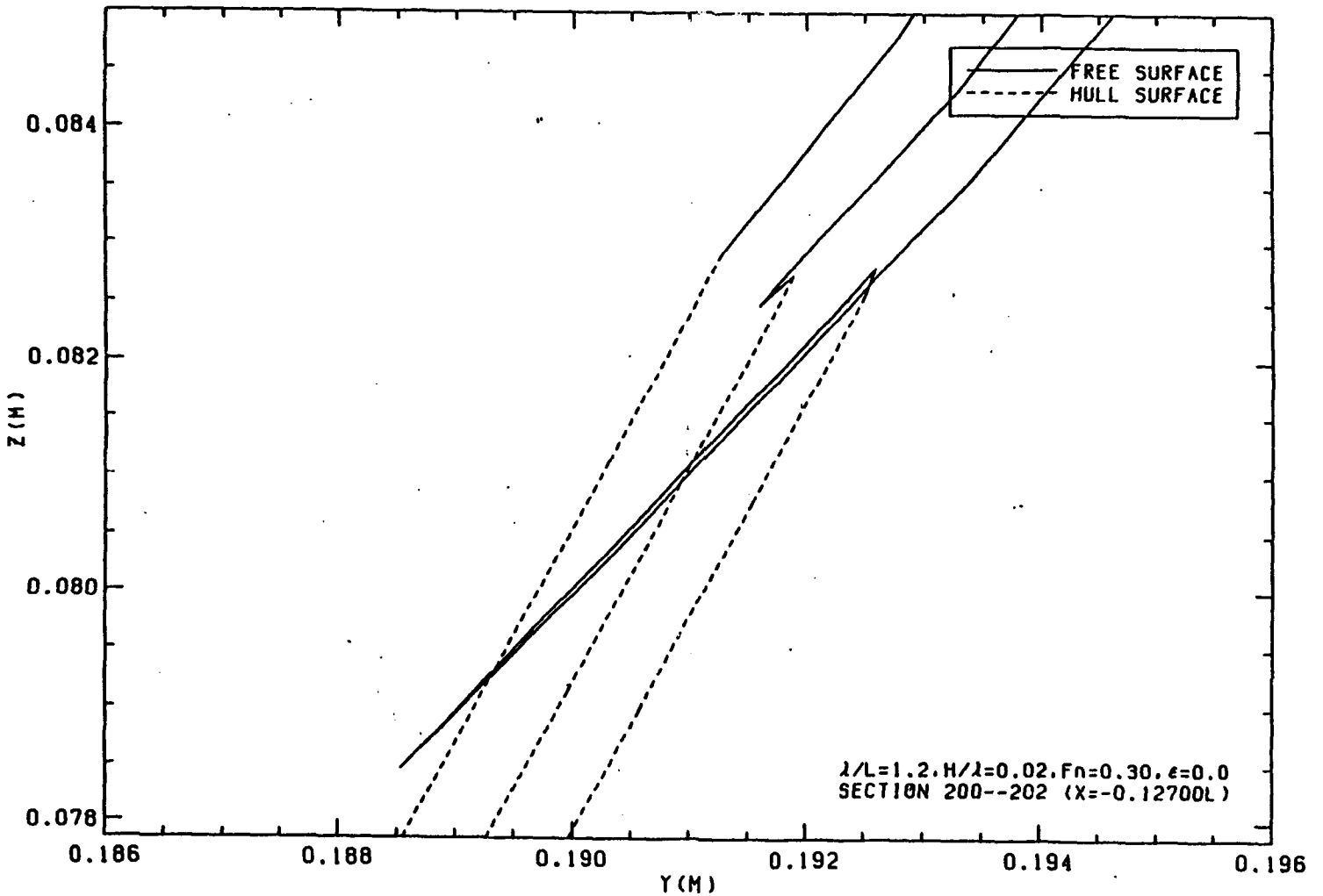

Figure 16 The magnified portion of water entering on deck in Figure 15

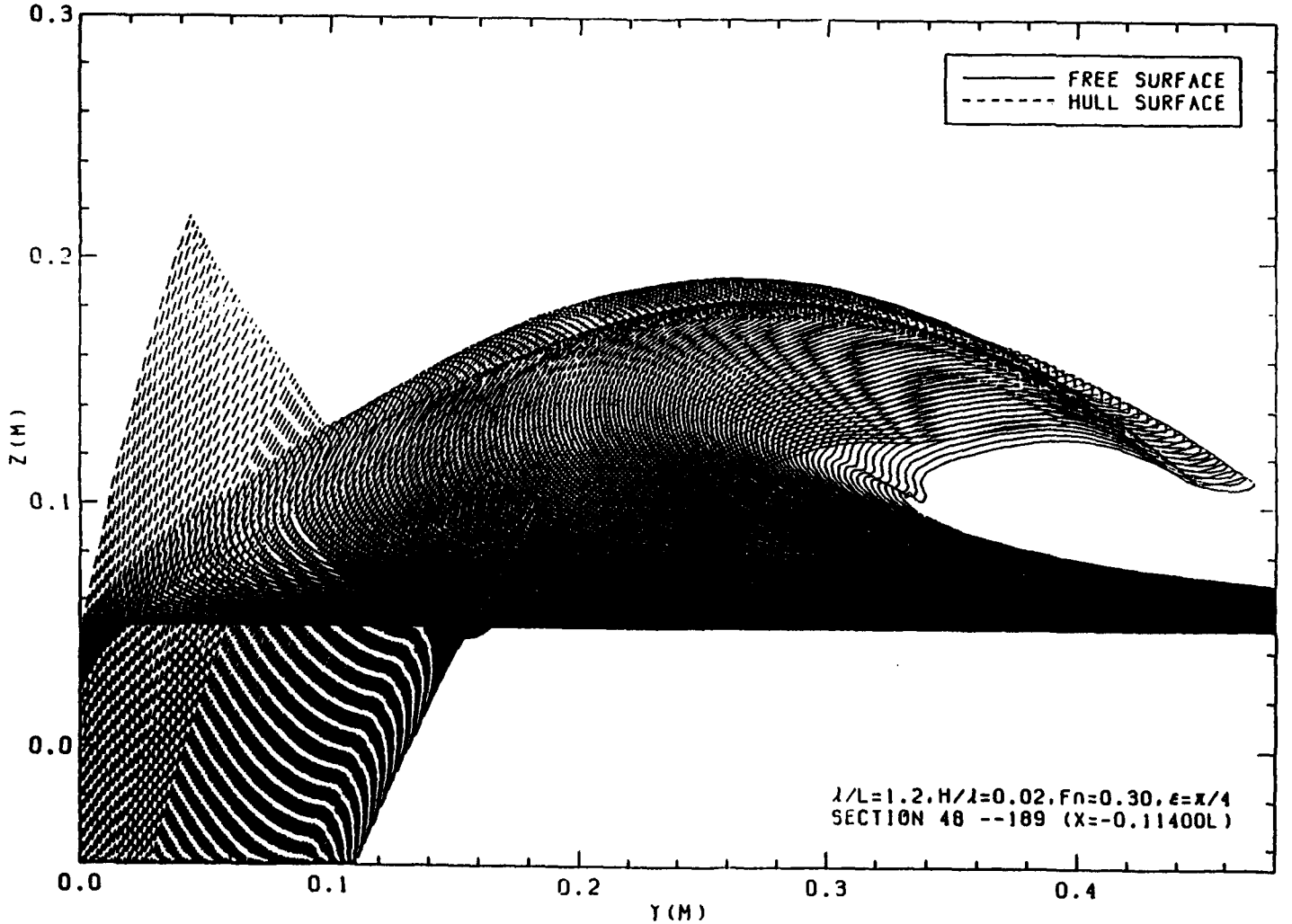

Figure 17 Wave elevation for a ship making heaving and pitching oscillation in sinusoidal head sea waves with l/λ=0.02 and $\varepsilon=\pi/4$

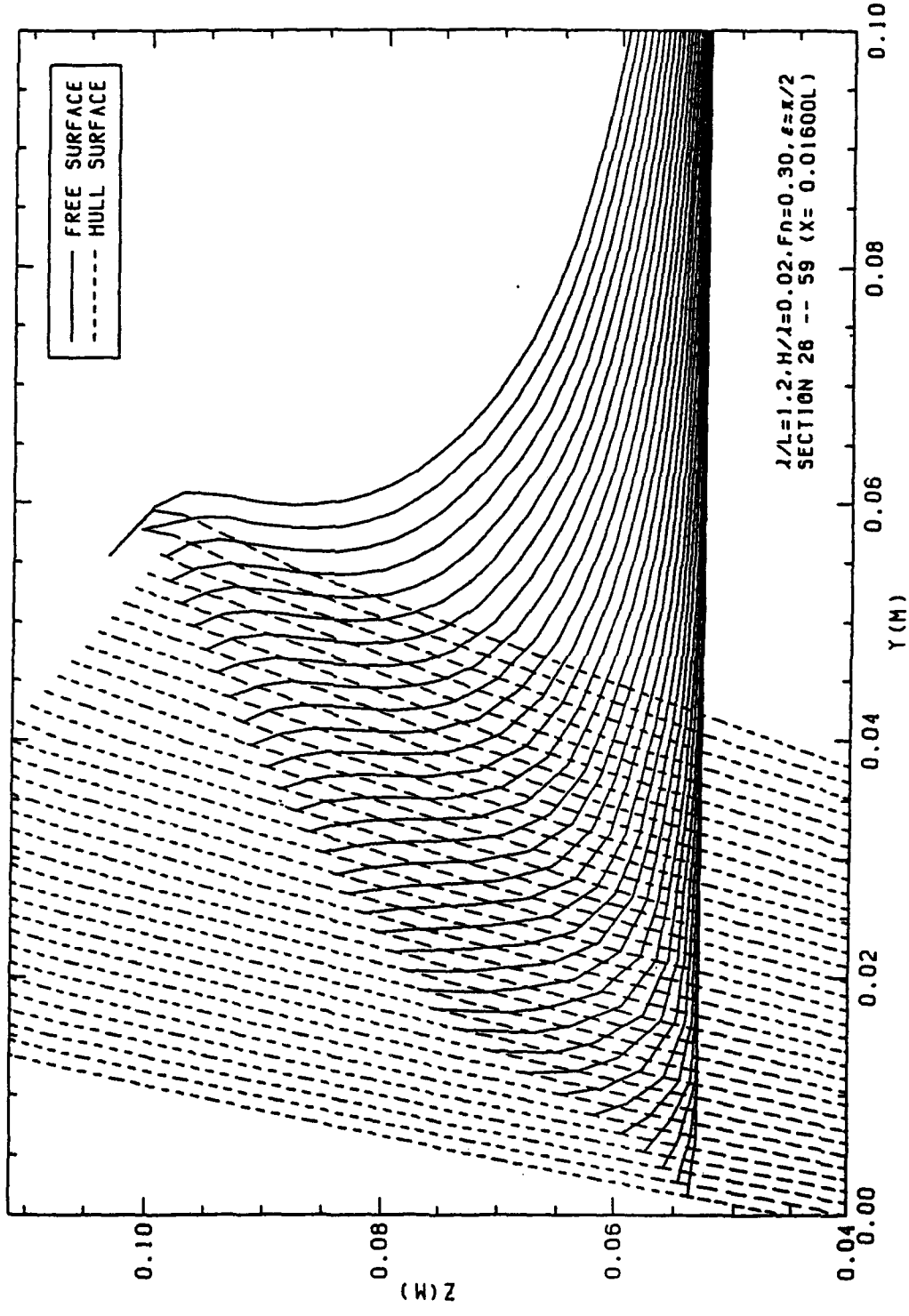

Figure 18 Wave elevation for a ship making heaving and pitching oscillation in sinusoidal head sea waves with H/λ=0.02 and $\varepsilon=\pi/2$

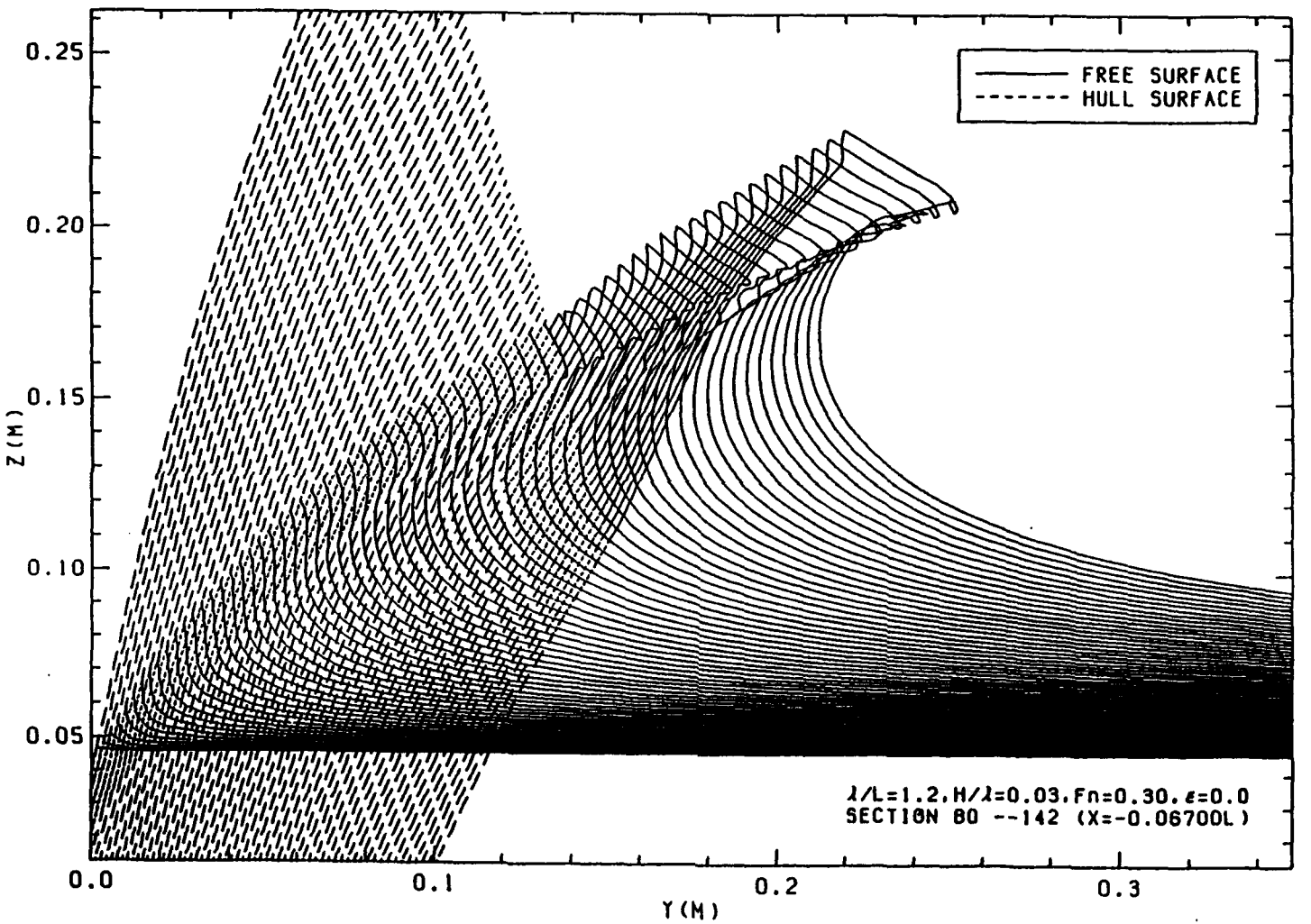

Figure 19 Wave elevation for a ship making heaving and pitching oscillation in sinusoidal head sea waves with H/λ=0.03 and ε=0.0

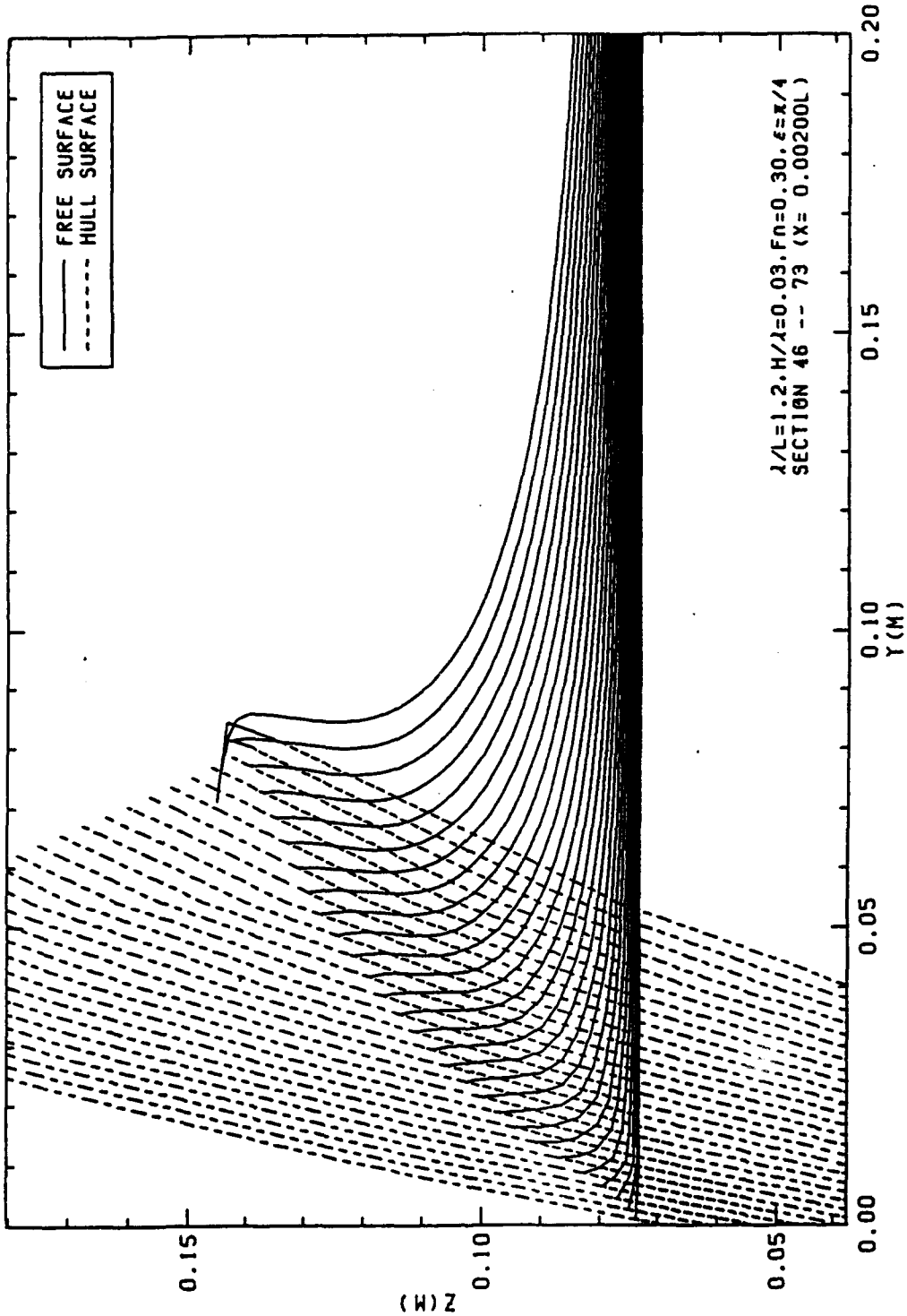

Figure 20 Wave elevation for a ship making heaving and pitching oscillation in sinusoidal head sea waves with H/λ=0.03 and $\varepsilon=\pi/4$

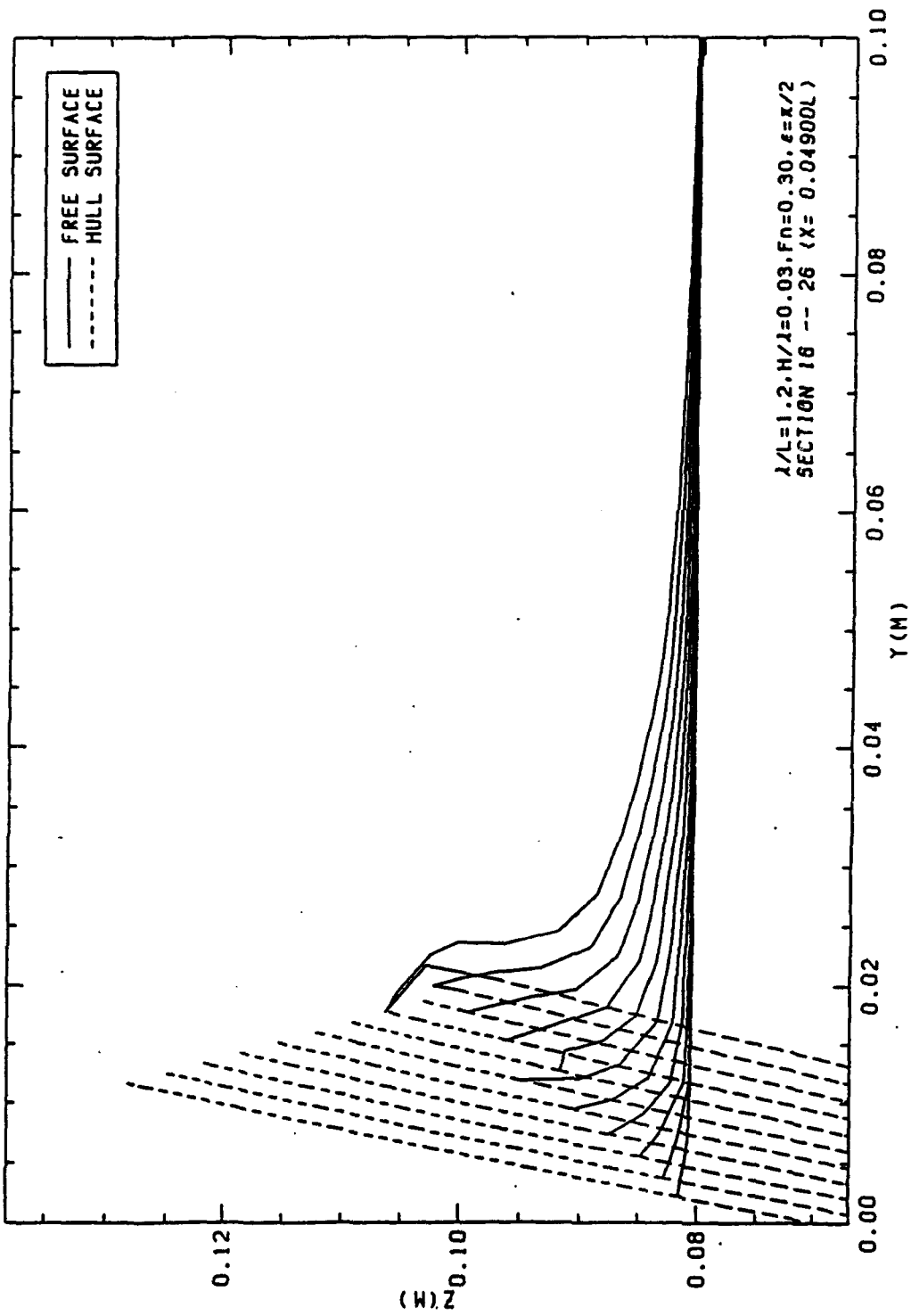

Figure 21 Wave elevation for a ship making heaving and pitching oscillation in sinusoidal head sea waves with H/λ=0.03 and $\varepsilon = \pi/2$.

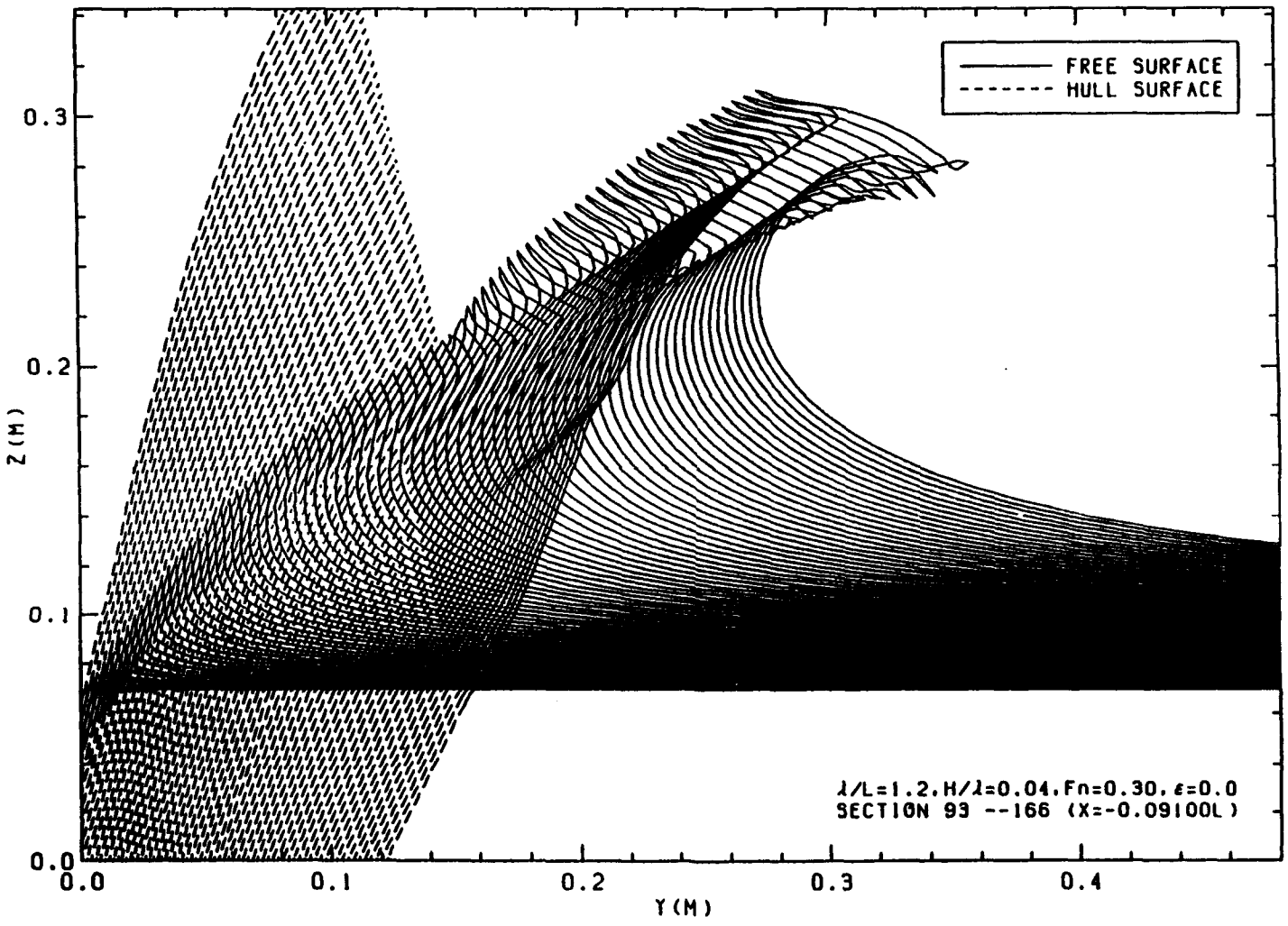

Figure 22 Wave elevation for a ship making heaving and pitching oscillation in sinusoidal head sea waves with H/λ=0.04 and ε=0.0

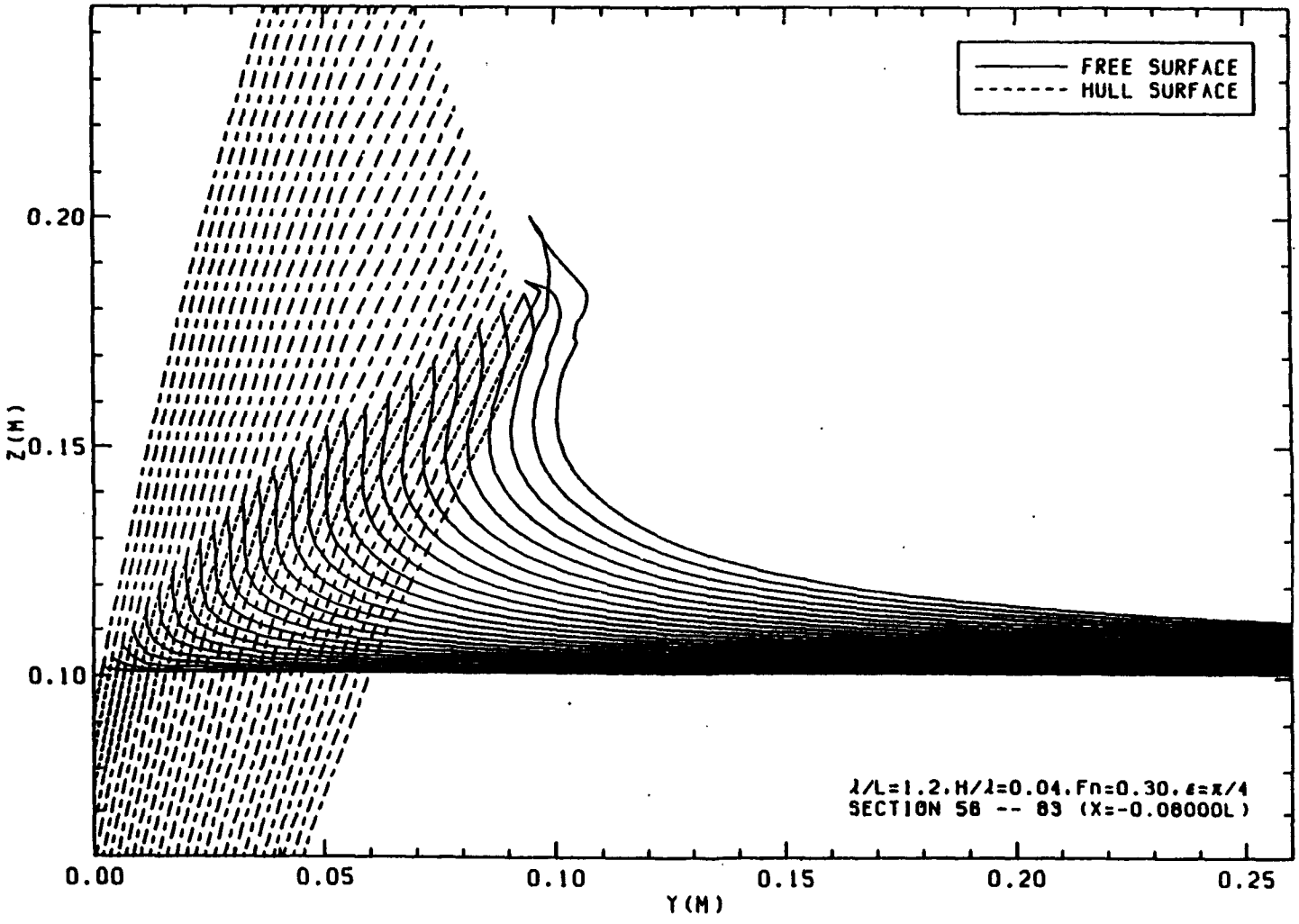

Figure 23 Wave elevation for a ship making heaving and pitching oscillation in sinusoidal head sea waves with H/λ=0.04 and $\varepsilon=\pi/4$

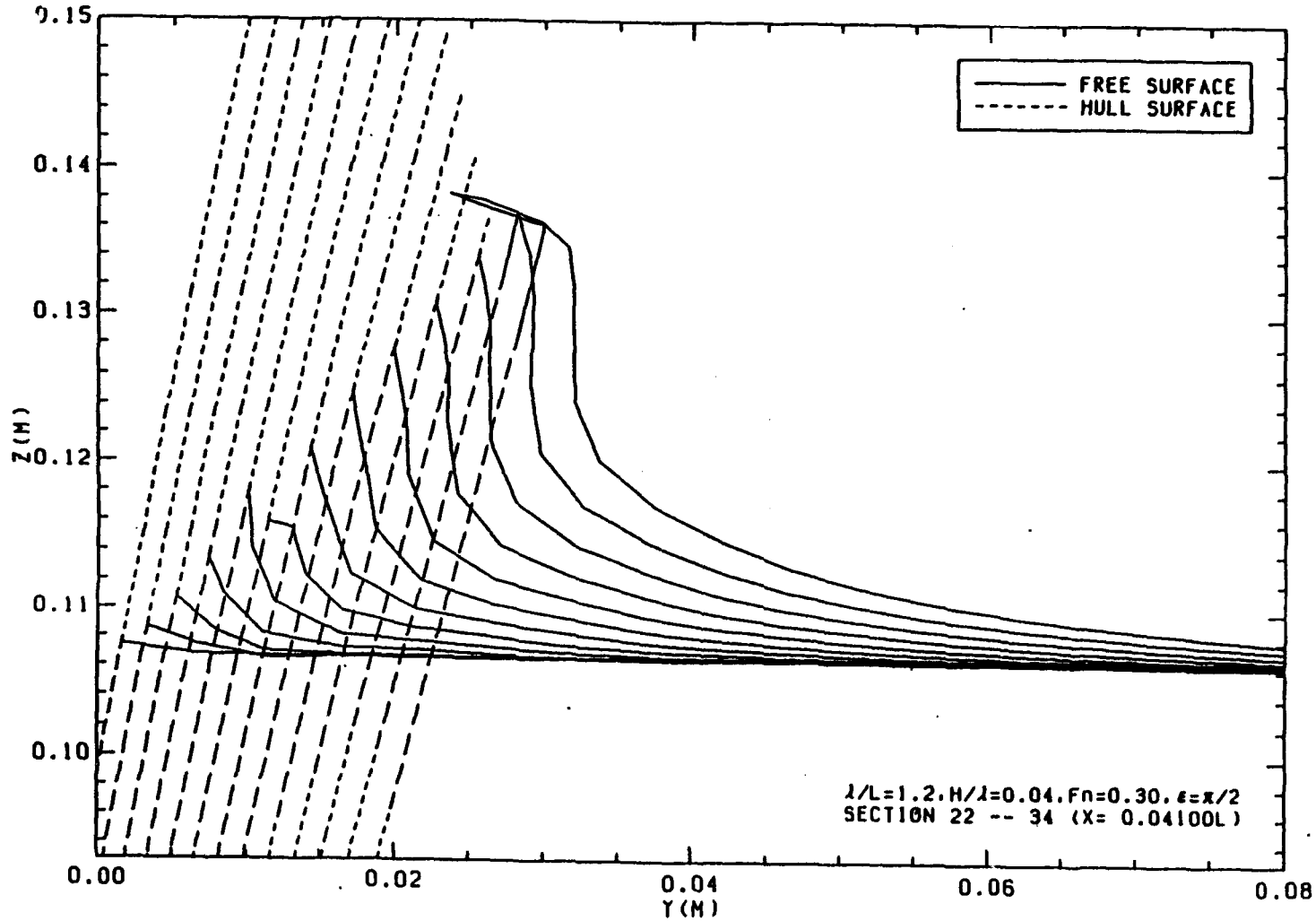

Figure 24 *Wave elevation for a ship making heaving and pitching oscillation in sinusoidal head sea waves with* H/λ=0.04 and $\varepsilon=\pi/2$